Legends for supplemental figures.

Supplemental Figure 1

Expression of PHD and HIF in control and *Phd2*$^{f/f}$*/aP2-Cre* mice.

A, Western blot analysis for PHD2 in heart, bone marrow derived macrophage (BMDM) and skeletal muscle (SKM from quadriceps femoris) in control and *Phd2*$^{f/f}$*/aP2-Cre* mice is shown. As a loading control, Western blotting for α-tubulin was performed. The same results were obtained in other independent experiments. n=3. **B,** The result of real-time qPCR analysis for adiponectin, F4/80 and *Phd2* in adipocyte rich fraction (Adipocyte) and stromal vascular fraction (SVF) in control and *Phd2*$^{f/f}$*/aP2-Cre* mice is shown in the bar graph. n=5. *P<0.05, **P<0.01 vs control. Adiponectin is specific for adipocytes and F4/80 is specific for macrophages. The results indicate that the two fractions are appropriately separated. **C**, The results of real-time qPCR analysis for Phd2 in SVF and Adipocytes from control and *Phd2*$^{f/f}$*/aP2-Cre* mice are shown. n=5. *P<0.05 vs control. N.S. not significant. **D**, The result of real-time qPCR analysis for Phd1 and Phd3 in white adipose tissue from control and *Phd2*$^{f/f}$*/aP2-Cre* mice is shown. n=3. **P<0.01 vs control. **E**. Statistical analysis of HIF-1α and HIF-2α expression in white adipose tissue from control and *Phd2*$^{f/f}$*/aP2-Cre* mice is shown. Western blot analysis for cAMP response element binding protein (CREB), a nuclear transcription factor, was used as a loading control. *P<0.05 vs control. n=3

Supplemental Figure 2

A. Glucose tolerance test in control and *Phd2*$^{f/f}$*/aP2-Cre* mice before high-fat diet feeding.

Glucose tolerance test was performed as indicated in the method. No significant difference was observed between control and *Phd2*$^{f/f}$*/aP2-Cre* mice.

B. Insulin tolerance test in control and *Phd2*$^{f/f}$*/aP2-Cre* mice after high-fat diet feeding for 6 weeks.

The results of insulin tolerance test in control and *Phd2*$^{f/f}$*/aP2-Cre* mice are indicated in actual glucose levels. n=6~7. **P<0.01, *P<0.05 vs control.

Supplemental Figure 3

Serum level of adipokines in control and *Phd2*$^{f/f}$*/aP2-Cre* mice.

Serum concentrations of MCP-1, IL-6, TNFα and adiponectin were determined by ELISA in high-fat diet fed control and *Phd2*$^{f/f}$*/aP2-Cre* mice. TNFα was not detectable in both mice and therefore the data are not shown. Although serum MCP-1 level is lower in *Phd2*$^{f/f}$*/aP2-Cre* mice, the difference was not statistically significant. n=6. N.S.; not significant.

Supplemental Figure 4.

Expression of protein in white adipose tissue (WAT) and skeletal muscle.

A, Western blot analysis shows expression of lactate dehydrogenase (LDH) a in WAT from control and *Phd2*$^{f/f}$*/aP2-Cre* mice. The bar graph shows the results of densitometric analysis. n=3. *P<0.05 vs control.

B, Western blot analysis shows phosphorylation of Akt and expression of Glut4 in skeletal muscle (quadriceps femoris). The bar graph shows the results of densitometric analysis. n=3. *P<0.05 vs control.

ORIGINAL ARTICLE

Inhibition of Neuregulin-1/ErbB Signaling in the Rostral Ventrolateral Medulla Leads to Hypertension through Reduced Nitric Oxide Synthesis

Ryuichi Matsukawa[1], Yoshitaka Hirooka[2], Koji Ito[1], and Kenji Sunagawa[1]

BACKGROUND

We recently reported that activation of neuregulin-1 (NRG-1)/ErbB signaling in the rostral ventrolateral medulla (RVLM) of the brainstem elicits sympathoinhibition and depressor effects, and ErbB2-type ErbB receptors are involved in the neurogenic mechanisms of hypertension. Nitric oxide (NO) in the RVLM also elicits sympathoinhibition and depressor effects. NRG-1 enhances NO synthase (NOS) expression in several tissues. Here, we tested the hypothesis that ErbB2 inhibition in the RVLM contributes to increasing blood pressure via modulating the effects of NOS.

METHODS

We measured the effects of chronic intracisternal infusion of an ErbB2 antagonist and local ErbB2 inhibition in the RVLM using RNA interference (ErbB2 siRNA) on blood pressure (BP), heart rate (HR), norepinephrine excretion (uNE), and NOS expression in the RVLM. The central effects of the ErbB2 antagonist or NRG-1β were investigated with or without chronic and acute prior administration of a NOS inhibitor.

RESULTS

Intracisternal infusion of the ErbB2 antagonist and ErbB2 siRNA increased BP, HR, and uNE; and reduced neuronal and endothelial NOS expression in the RVLM. Further, prior systemic administration of a NOS inhibitor abolished the pressor response to intracisternal infusion of an ErbB2 antagonist in awake rats. Prior injection of a NOS inhibitor or γ-aminobutyric acid–A receptor antagonist into the RVLM attenuated the depressor response to NRG-1 in anesthetized rats.

CONCLUSIONS

These findings indicate that inhibition of ErbB2 expression in the RVLM leads to hypertension, at least in part, by reducing NO synthesis and inhibiting γ-aminobutyric acid activity. NRG-1/ErbB signaling in the RVLM might exist upstream of NO synthesis.

Keywords: blood pressure; ErbB2; hypertension; neuregulin-1; nitric oxide synthase, RVLM; sympathetic nervous system.

doi:10.1093/ajh/hps005

Neuregulin-1 (NRG-1) binds to the extracellular domain of the ErbB family of tyrosine kinase receptors, including ErbB2, ErbB3, and ErbB4. NRG-1/ErbB signaling is involved in cell proliferation and differentiation in many tissues.[1–3] NRG-1 and ErbB receptors are also distributed in the central nervous system and activate intracellular signaling pathways affecting synaptic function, neurite outgrowth, and survival of neurons and glia.[4–8] We recently reported that NRG-1 stimulation in the rostral ventrolateral medulla (RVLM) of the brainstem, an important region involved in cardiovascular regulation,[9,10] elicits sympathoinhibition and depressor effects.[11] In contrast, blockade of ErbB2 and ErbB4 in the RVLM elicits sympathoexcitation and pressor effects. These findings suggest that NRG-1/ErbB signaling in the RVLM comprises an antihypertensive system with sympathoinhibition.[11] Furthermore, ErbB2 expression levels in the brainstem are reduced in spontaneously hypertensive rats compared to Wistar Kyoto (WKY) rats, and both the depressor response to NRG-1 and the pressor response to the ErbB2 antagonist are attenuated in spontaneously hypertensive rats,[11] suggesting that NRG-1/ErbB signaling in the RVLM is impaired in spontaneously hypertensive rats due to reduced ErbB2 expression. Central NRG-1/ErbB signaling in the RVLM has sympathoinhibitory effects, and impaired NRG-1/ErbB signaling due to reduced ErbB2 expression contributes to the neural mechanisms of hypertension. In NRG-1/ErbB signaling, ErbB2 has a key role in the neural mechanisms of hypertension. The precise mechanism underlying the increase in sympathetic nerve activity due to decreased ErbB2 function, however, has been unclear.

Nitric oxide (NO) in the RVLM contributes to the regulation of sympathetic tone and blood pressure.[12–14] NO is synthesized from its precursor, L-arginine, by endogenous NO synthase (NOS). There are three NOS isoforms, including neuronal NOS (nNOS), endothelial NOS (eNOS), and

Correspondence: Yoshitaka Hirooka (hyoshi@cardiol.med.kyushu-u.ac.jp)

Initially submitted May 21, 2012; date of first revision July 24, 2012; accepted for publication July 27, 2012.

[1]Department of Cardiovascular Medicine, Kyushu University Graduate School of Medical Sciences, Fukuoka, Japan; [2]Department of Advanced Cardiovascular Regulation and Therapeutics, Kyushu University Graduate School of Medical Sciences, Fukuoka, Japan.

inducible NOS (iNOS). All three isoforms generate NO from L-arginine, but have distinct functional and structural features.[15] Increased NO in the RVLM by eNOS overexpression induces depressor effects and inhibits central sympathetic outflow by increasing the release of γ-aminobutyric acid (GABA).[16–18] NO regulates sympathetic nerve activity partly by modulating GABAergic neurotransmission. On the other hand, several studies report that NRG-1 interacts with NO. For example, NRG-1 augments nNOS expression in the cerebellum[19] and eNOS expression in cardiomyocytes.[20,21] It is not known, however, whether NRG-1/ErbB signaling in the RVLM influences the effects of NO and GABA.

The aim of the present study was to clarify whether ErbB2 inhibition in the RVLM contributes to increasing blood pressure via modulation of NO and GABA. Expression levels of nNOS and eNOS in the RVLM were evaluated when ErbB2 in the RVLM was inhibited using pharmacologic and genetic methods. We investigated the effects of NOS inhibition in the RVLM on the cardiovascular effects of NRG/ErbB signaling in both anesthetized and awake rats.

METHODS

This study was reviewed and approved by the Committee on Ethics of Animal Experiments, Kyushu University Graduate School of Medical Sciences, and performed according to the Guidelines for Animal Experiments of Kyushu University.

Animals

The study was performed using male WKY rats (12 weeks old, n = 65). All animals were purchased from SLC (Fukuoka, Japan).

Continuous intracisternal infusion of an ErbB2 antagonist

Chronic intracisternal infusion of an ErbB2 antagonist (AG825: 0.1 mmol/L, 0.25 μL/h) was performed according to the following protocols: (i) the first group received continuous infusion of AG825 for 2 weeks using a subcutaneously implanted mini-osmotic pump (Alzet model 1002; Durect Corporation). The second group received continuous intracisternal infusion of the vehicle (cerebrospinal fluid (a-CSF), 0.25 μL/h) for 2 weeks using the same type of implanted pump. The surgical procedures were performed as described previously.[22,23] Infusion was stopped in both groups 14 days after initiation. Arterial pressure (AP) and heart rate (HR) were measured using a radiotelemetry system for 21 days. Expression of ErbB2, phosphorylated ErbB2, nNOS, and eNOS in the RVLM of WKY rats on day 7 after the initiation of intracisternal infusion was evaluated using Western blot methods. Urinary norepinephrine (uNE) concentrations were measured on days 0, 7, 14, and 21 after the start of the intracisternal infusion of the ErbB2 antagonist and uNE excretion was calculated as described previously.[16,22] (ii) All rats received NG-nitro-L-arginine methyl ester (L-NAME; Cayman Chemical, Ann Arbor, MI) in their drinking water (1.0 mg/mL) for 2 weeks, as previously described.[24,25] At the concentration administered, the daily intake of L-NAME was 30 to 40 mg. Rats treated with L-NAME were randomly separated into two groups. Continuous infusion of AG825 (0.1 mmol/L, 0.25 μL/h) or vehicle (a-CSF, 0.25 μL/h) was started on day 7 after the start of L-NAME treatment and continued for 7 days. Measurement of AP and HR using the radiotelemetry system was started 3 days before L-NAME treatment. We measured the uNE concentration on days 0 and 14 after the initiation of L-NAME treatment and calculated uNE excretion.

Radiotelemetric monitoring of BP and HR

The UA-10 telemetry system (Data Sciences International, St. Paul, MN) was used to measure mean arterial pressure (MAP) and HR. The surgical procedure used in the study was similar to that described in previous studies.[16,22] MAP and HR values were continuously recorded for 10 to 30 min every day in the morning using a multichannel amplifier and signal converter.

In vivo Small-interference RNA technique

The ErbB2 small-interference RNA (siRNA) sequence was determined as described in a previous study.[11,26] Specific ErbB2 siRNA and scrambled siRNA as a control (siControl) were purchased from Koken (Tokyo, Japan). We also used the in vivo siRNA delivery kit AteloGene (Koken) for stable local delivery of the siRNA into the RVLM, as previously described.[11,26,27] We confirmed the successful inhibition of ErbB2 expression and an increase in MAP and HR 1 day after ErbB2 siRNA administration in a recent study.[11] Thus, before and 1 day after the siRNA injection, we evaluated nNOS, eNOS, and ErbB2 expression in the RVLM using Western blot methods. MAP and HR were also measured at the same time using a radiotelemetry system.

Western blot analysis

Rabbit immunoglobulin G (IgG) monoclonal antibodies against ErbB2 (1:1000), phosphorylated ErbB2 (1:1000), nNOS (1:1000), and eNOS (1:1000) were used as the primary antibodies. All antibodies were purchased from Santa Cruz Biochemical (Santa Cruz, CA). The animals were anesthetized using sodium pentobarbital (100 mg/kg; intraperitoneal injection) and perfused transcardially with phosphate-buffered saline. The brains were removed quickly. RVLM tissues, defined according to a rat brain atlas, were obtained as previously described.[28] The tissues were homogenized and then sonicated in a lysis buffer containing 40 mmol/L 4-(2-hydroxyethyl)-1-piperazine ethanesulphonic acid, 1% Triton X-100, 10% glycerol, 1 mmol/L phenylmethanesulfonyl fluoride, and 1 protease inhibitor cocktail tablet (Roche Diagnostics, Indianapolis, IN). The tissue lysate was centrifuged in a microcentrifuge at 6,000 rpm for 5 min at 4 °C. The lysate was collected, and the protein concentration determined using a bicinchoninic acid protein assay kit (Pierce Chemical, Rockford, IL). Aliquots of protein (50 μg) from each sample were

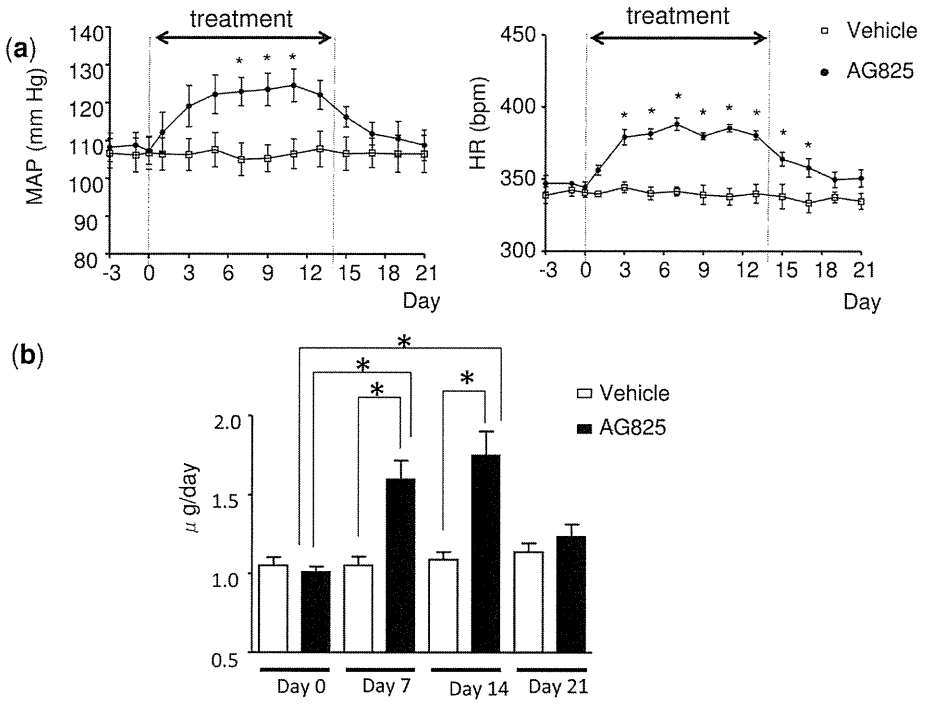

Figure 1. Effect of chronic intracisternal infusion of an ErbB2 receptor antagonist on MAP, HR, and sympathetic nerve activity. (**a**) Effect of chronic intracisternal infusion of AG825 on MAP and HR. *$P < 0.05$; n = 5 per infusion. (**b**) Group data for uNE. $P < 0.05$; n = 5 per infusion. Values are expressed as mean ± SEM. Abbreviations: HR, heart rate; MAP, mean arterial pressure; uNE, urinary norepinephrine excretion.

separated on a 7.5% sodium dodecyl sulfate-polyacrylamide gel. Subsequently, separated proteins were transferred onto polyvinylidene difluoride membranes (Immobilon-P membrane; Millipore, Billerica, MA). The membranes were incubated with rabbit IgG monoclonal antibody for 24 to 48 h. The membranes were then washed and incubated with horseradish peroxidase–conjugated horse antirabbit IgG antibody (1:10,000) for 40 min. Immunoreactivity was detected using autoradiography with enhanced chemiluminescence and a Western blotting detection kit (GE Healthcare, Tokyo, Japan).

Microinjection studies

Animals were anesthetized using sodium pentobarbital and AP and HR were measured as described previously.[11] We identified the RVLM region by injecting a small dose of L-glutamate as previously described.[16] Microinjections into the RVLM were made according to the following protocol: (i) unilateral microinjection of NRG-1β (2.5 pmol in 50 nL; BioVision, Mountain View, CA) 10 min after unilateral injection of NG-monomethyl-L-arginine (L-NMMA, 50 pmol in 50 nL; Cayman Chemical) in WKY rats; and (ii) unilateral microinjection of NRG-1β (2.5 pmol in 50 nL) 5 min after unilateral injection of the GABA-A receptor antagonist bicuculline (100 pmol in 50 nL; Santa Cruz Biochemical) in WKY rats. Dosages of reagents were determined based on previous studies.[16,29] In microinjection experiments, we confirmed the RVLM region histologically after the experiments by dye injection.

Statistical analysis

All values are expressed as mean ± SEM. Changes in the MAP and HR values during the siRNA study and expression of ErbB2, phosphorylated ErbB2, and eNOS were compared using a paired *t* test. Intergroup differences in MAP and HR values obtained using the radiotelemetry system were compared using 2-way analysis of variance. Intergroup differences in MAP and HR values during the microinjection study, uNE values for 24 h, and ErbB2 expression in the siRNA study were compared using 1-way analysis of variance. In the analysis of variance, comparisons between any 2 mean values were performed using Bonferroni's correction for multiple comparisons. Differences were considered significant when the *P* value was less than 0.05.

RESULTS

Chronic effects of ErbB2 inhibition in the brainstem on BP, HR, and uNE excretion with intracisternal infusion of the ErbB2 antagonist

Chronic intracisternal infusion of AG825 increased MAP and HR. In the AG825-treated rats, increases in MAP and HR were detected from day 1 after the initiation of treatment. Increases in MAP were significant between days 7 and 11, while increases in HR were significant between days 3 and 17. In contrast, these variables did not change in the vehicle-treated rats (Figure 1a). Increases in the uNE levels on days 7 and 14 were significantly greater in the AG825-treated rats than in the vehicle-treated rats (Figure 1b).

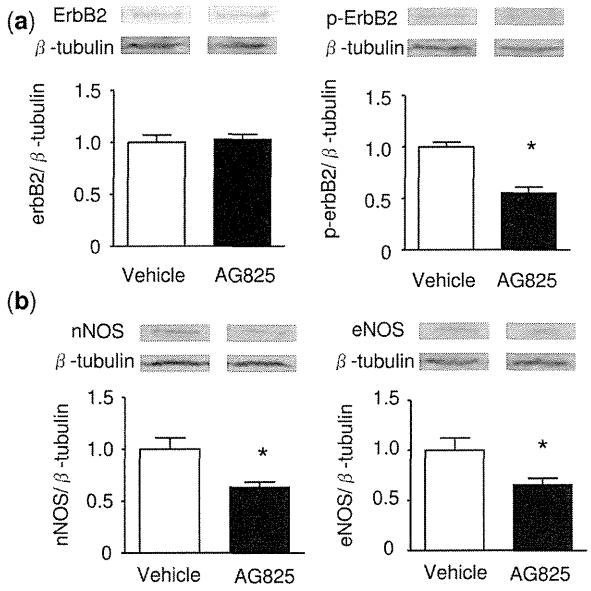

Figure 2. Effect of central ErbB2 receptor inhibition on expression levels of ErbB2, phosphorylated ErbB2, nNOS, and eNOS in the RVLM at 7 days after initiation of treatment. The representative bands were cut from separated lanes from same membrane. (**a**) Representative Western blots of ErbB2 and phosphorylated ErbB2 in the RVLM of AG825-treated or vehicle-treated Wistar-Kyoto rats. (**b**) Representative Western blots of nNOS and eNOS in the RVLM of AG825-treated or vehicle-treated WKY rats. The densitometric average was normalized to values obtained from the analysis of β-tubulin as an internal control. Expression is shown relative to that in control, which was assigned a value of 1. Values are expressed as mean ± SEM. *$P < 0.05$ (vs. control, n = 5 for each). *Abbreviations: eNOS, endothelial nitric oxide synthase; nNOS, neuronal nitric oxide synthase; RVLM, rostral ventrolateral medulla.*

Effects of ErbB2 inhibition in the brainstem on nNOS and eNOS expression levels in the RVLM

ErbB2 protein expression levels on day 7 did not differ significantly between AG825-treated rats and vehicle-treated rats. Phosphorylated ErbB2 protein expression levels were lower in AG825-treated rats than in vehicle-treated rats on day 7 (Figure 2a). Both nNOS and eNOS protein expression levels in the RVLM were significantly lower in AG825-treated rats than in vehicle-treated rats on day 7 (Figure 2b).

Effects of local ErbB2 inhibition in the RVLM on nNOS and eNOS expression levels

Administration of ErbB2 siRNA into the RVLM successfully inhibited ErbB2 expression levels in the RVLM and significantly increased MAP and HR on day 1 after treatment (Figure 3b,3c). Baseline MAP and HR before administration of the siRNA were as follows (control vs. ErbB2 siRNA): MAP, 95.4 ± 5.4 vs. 93.3 ± 5.7 mm Hg; HR, 313.7 ± 9.1 vs. 308.7 ± 8.9 beats/min. Both nNOS and eNOS protein expression levels in the RVLM were significantly lower in ErbB2 siRNA-treated rats than in control siRNA-treated rats on day 1 after treatment (Figure 3a).

Effect of chronic blockade of NOS on the pressor response to chronic intracisternal infusion of an ErbB2 antagonist

MAP and HR significantly increased during L-NAME treatment. Excretion of uNE was also increased on day 14 compared to levels before treatment (Figure 4a,4b). Intracisternal infusion of AG825, however, did not induce further changes in MAP, HR, or uNE excretion (Figure 4a,4b).

Effect of blockade of NOS and GABA-A receptors in the RVLM on the depressor response to NRG-1

The baseline MAP increased from 93.3 ± 5.6 before NRG-1β injection to 115.9 ± 7.5 mm Hg after the L-NMMA injection, and the HR slightly increased from 319.6 ± 10.3 to 324.2 ± 10.1 beats/min. Prior injection of L-NMMA into the RVLM significantly ($P < 0.01$) attenuated the depressor response to NRG-1β in anesthetized WKY rats (Figure 4c). The baseline MAP increased from 94.3 ± 7.1 before NRG-1β injection to 119.4 ± 6.2 mm Hg after the bicuculline injection, and the HR slightly decreased from 314.1 ± 12.0 to 310.4 ± 13.2 beats/min. Prior injection of bicuculline into the RVLM also significantly ($P < 0.01$) attenuated the depressor response to NRG-1β (Figure 4c). The effects of L-NMMA and bicuculline on MAP and HR were not significantly different.

DISCUSSION

The results of the present study are the first to suggest that attenuation of ErbB2 activity in the RVLM causes hypertension by reducing NOS expression. Chronic intracisternal infusion of an ErbB2 antagonist, AG825, and administration of ErbB2 siRNA into the RVLM induced increases in BP and HR in awake rats and reduced nNOS and eNOS in the RVLM. Based on these findings, NRG-1/ErbB signaling in the RVLM is likely upstream of NOS, because prior NOS inhibition abolished pressor and tachycardic responses

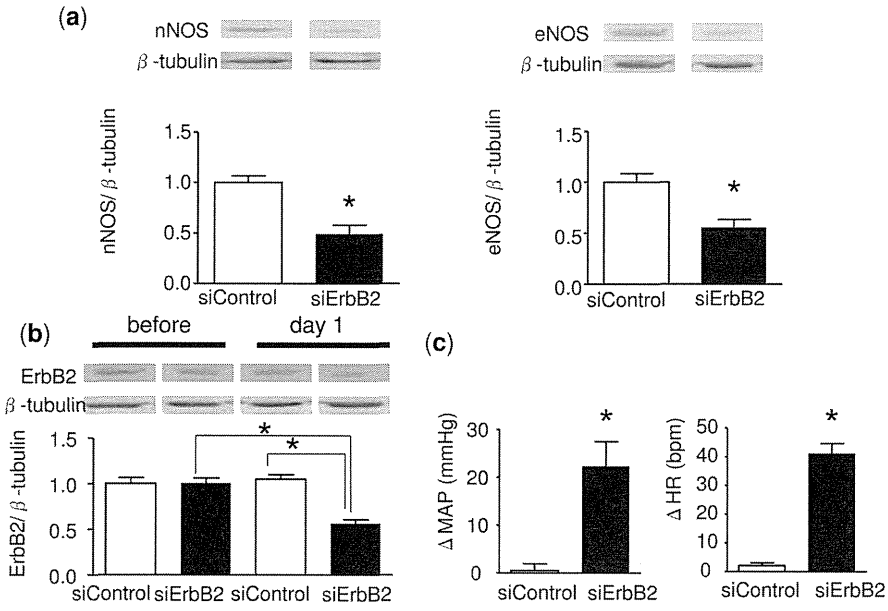

Figure 3. Effect of local administration of ErbB2 siRNA (siErbB2) and siControl into the RVLM of Wistar Kyoto rats on nNOS and eNOS expression in the RVLM. The representative bands were cut from separated lanes from same membrane. (**a**) Representative Western blot of nNOS and eNOS expression in the RVLM at 1 day after starting the treatment. The densitometric average was normalized to values obtained from the analysis of β-tubulin as an internal control. Expression is shown relative to that of siControl, which was assigned a value of 1. Values are expressed as mean ± SEM. *$P < 0.05$ (vs. siControl, n = 5 for each). (**b**) Representative Western blot of ErbB2 in the RVLM in the siErbB2 treatment and siControl treatment groups before and at 1 day after starting treatment. Expression is shown relative to that in siControl before treatment, which was assigned a value of 1. Values are expressed as mean ± SEM. *$P < 0.05$ (vs. siControl before the treatment, n = 5 for each). (**c**) Effect of local administration of siErbB2 and siControl into the RVLM on MAP and HR at 1 day after starting treatment. Values are expressed as mean ± SEM. *$P < 0.05$ (vs. siControl, n = 5 for each). Abbreviations: eNOS, endothelial NOS; HR, heart rate; MAP, mean arterial pressure; nNOS, neuronal nitric oxide synthase; RVLM, rostral ventrolateral medulla; siControl, control siRNA; siRNA, small-interference RNA.

to chronic intracisternal infusion of an ErbB2 antagonist in awake WKY rats. In addition, the depressor response to NRG-1 in the RVLM was attenuated by prior injection of a NOS inhibitor in anesthetized rats. Thus, an attenuation of ErbB2 in the RVLM might contribute to the neurogenic mechanisms of hypertension by reducing NOS expression.

Central administration of an ErbB2 antagonist reduced both nNOS and eNOS expression in the RVLM. Furthermore, central ErbB2 inhibition elicited hypertension and tachycardia with an increase in sympathetic activity by reducing NOS expression. Therefore, we suggest that NRG-1/ErbB signaling might be upstream of NOS, at least in a part, in the RVLM. This suggestion is supported by the finding that prior systemic administration of a NOS inhibitor, which also inhibits brain NOS,[30] abolished the pressor and tachycardic response to chronic intracisternal infusion of an ErbB2 antagonist. Systemic L-NAME treatment increased baseline AP and HR. A decrease in the HR in the early phase of L-NAME treatment might be caused by baroreflex. The possibility that these changes in baseline AP and HR affect abolishment of the effect of AG825 cannot be ruled out. Further studies are needed to clarify this issue. Taken together, our findings indicate that ErbB2 inhibition reduces NOS expression in the RVLM, thereby raising the blood pressure and HR by increasing sympathetic activity.

In rats with chronic intracisternal infusion of AG825, phosphorylated ErbB2 levels, but not ErbB2 expression itself, were reduced in the RVLM. AG825 is a selective ATP-competitive inhibitor of the tyrosine kinase activity of ErbB2 autophosphorylation.[31,32] Our findings are thus consistent with these characteristics of AG825. The possibility that intracisternal infusion of AG825 affects other brainstem nuclei, thereby inducing hypertension and tachycardic responses, however, cannot be ruled out by our findings. Thus, we injected ErbB2 siRNA into the RVLM for site-specific inhibition. This treatment also reduced nNOS and eNOS expression in the RVLM. In addition, microinjection of NRG-1, which activates ErbB2, into the RVLM of anesthetized WKY rats elicited depressor and bradycardic responses. Prior injection of a NOS inhibitor into the RVLM attenuated the responses to NRG-1. Taken together, our findings suggest that inhibition of endogenous ErbB2 in the RVLM elicits pressor and tachycardic responses by increasing sympathetic activity due to the reduction of NOS.

GABA is a major inhibitory neurotransmitter that reduces the activity of RVLM neurons. For example, NO activates 3′,5′-cyclic guanosine monophosphate and 3′,5′-cyclic guanosine monophosphate–stimulated protein kinase G, which leads to GABA release.[33] The increase in NOS expression in the RVLM elicits a depressor response via augmenting GABA release.[12,16,17] The depressor response to NRG-1 in the RVLM is attenuated by prior injection of a GABA-A receptor antagonist in WKY rats. This finding is consistent with the results of our recent study using Wistar rats, suggesting that NRG-1 in the RVLM elicits a depressor response via enhancing GABA activity.[11] Furthermore, the degree of inhibition induced by either an NOS inhibitor or a GABA-A receptor antagonist was not significantly different. This

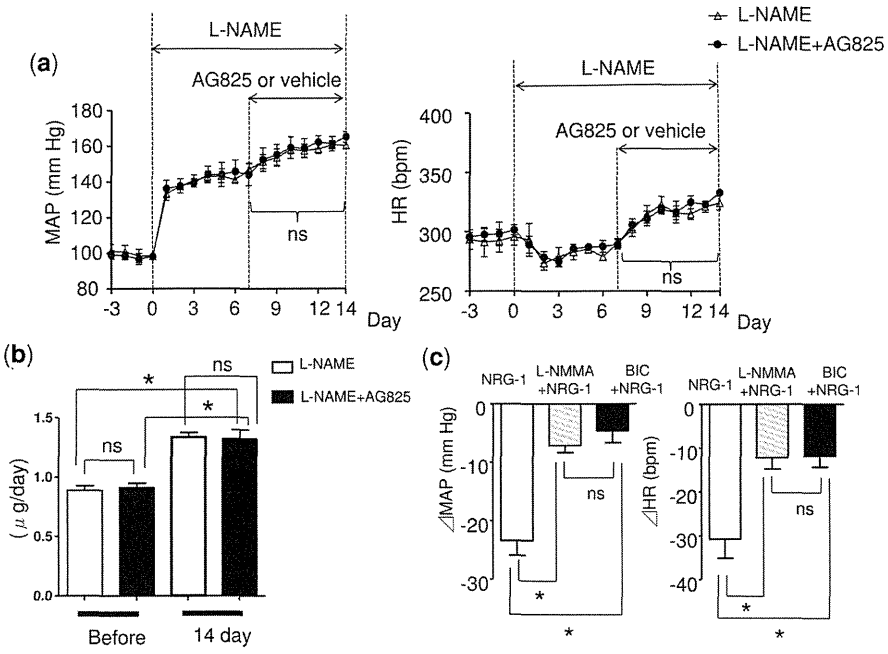

Figure 4. The effect of prior oral administration of L-NAME on the pressor and tachycardic responses to chronic intracisternal administration of AG825 and the effect of acute prior microinjection of L-NMMA or bicuculline on the depressor and bradycardic responses to acute microinjection of NRG-1β into the RVLM. (**a**) The changes in MAP, HR, and (**b**) uNE induced by chronic intracisternal administration of AG825 after oral administration of L-NAME. L-NAME: L-NAME and vehicle-treated rats. L-NAME + AG825: L-NAME and AG825-treated rats. (**c**) Comparisons of the responses of MAP and HR to microinjection of NRG-1β into the RVLM with or without prior injection of L-NMMA or bicuculline. Values are expressed as mean ± SEM. *$P < 0.05$ (n = 5 for each). NRG-1: microinjection of only NRG-1β. NRG-1 + L-NMMA: microinjection of NRG-1β after injection of L-NMMA. NRG-1 + BIC: microinjection of NRG-1β after injection of BIC. Abbreviations: BIC, bicuculline; HR, heart rate; L-NAME, NG-nitro-L-arginine methyl ester; L-NMMA, NG-monomethyl-L-arginine; MAP, mean arterial pressure; NRG-1, neuregulin-1; ns, not significant; RVLM, rostral ventrolateral medulla; uNE, urinary norepinephrine excretion.

finding suggests that NRG-1 in the RVLM elicits a depressor response mainly by augmenting GABA activity via an increase in NOS expression. NRG-1 in the RVLM decreases blood pressure by enhancing NOS mediated GABA action. Kishi *et al.* previously demonstrated that overexpression of eNOS in the RVLM increased GABA levels by *in vivo* microdialysis.[16,34] NRG-1 enhances presynaptic GABA release in hippocampal neurons.[34] Taken together with previous findings, the increased GABA activity induced by NRG-1 in the present study might be due to an increase in NOS expression. Further studies are needed to determine whether NRG-1 acts presynaptically or postsynaptically *in vivo*. Increased activity in the RVLM is one of the factors of chronic sympathetic hyperactivity in many forms of hypertension. NOS-mediated GABAergic activity has inhibitory effects on RVLM neurons.[12,16,17] NRG-1/ErbB signaling induces NOS-mediated GABAergic inhibition of RVLM neurons.

We did not investigate the precise mechanism(s) by which NRG/ErbB activation induces NOS expression and phosphorylation in the present study. NRG-1/ErbB signaling activates many important intracellular mechanisms, such as extracellular signal-regulated kinase 1/2, Akt,[1–3] indicating that there are complex interactions downstream of this signaling. Also, we focused on the role of ErbB2 receptors in the RVLM in the present study because we previously demonstrated that ErbB2 receptors are responsible for central BP regulation and decreased ErbB2 receptors are related to hypertensive mechanisms.[11] It is possible that NRG-1 in the RVLM influences not only GABAergic but also glutamatergic transmission, because we also demonstrated that NRG-1 attenuates the response to glutamate in the RVLM.[11] The effect of NO in the RVLM is controversial. Chan *et al.* reported that endogenous NO produced by nNOS increases blood pressure in anesthetized rats.[35] They performed acute pharmacological experiments under anesthesia, however, and did not check changes in chronic nNOS expression levels. We consider that the amount of NO produced and oxidative stress might be involved in the discrepancy, as discussed in our previous paper,[36] although we still do not have a clear explanation for the differences between their results and ours. Nevertheless, the findings in the present study suggest that NOS is critically involved in NRG/ErbB signaling. Further studies are required to clarify the extent to which this signaling pathway through NO plays a role in neural mechanisms of hypertension as well as blood pressure regulation.

NRG-1 and ErbB2 are distributed ubiquitously in the brain, although there might be some differences in the density in various areas of the brain.[6,7] We did not examine the difference in ErbB2 distribution in the brain in the present study. This type of signaling in other brain nuclei might have a different role in blood pressure regulation. Further studies are needed to clarify the role of this type of signaling in other brain nuclei in the mechanisms underlying neurogenic hypertension.

In conclusion, our findings indicate that NRG-1/ErbB signaling in the RVLM is upstream of NOS and GABA.

Attenuating ErbB2 in the RVLM, at least in part, reduces NOS-mediated GABA activity, leading to increased sympathetic activity and BP elevation.

ACKNOWLEDGMENTS

This study was supported by Grants-in-Aid for Scientific Research from the Japan Society for the Promotion of Science and a Grant from the Mitsubishi Pharma Research Foundation.

DISCLOSURE

The authors declared no conflict of interest.

REFERENCES

1. Lemmens K, Doggen K, De Keulenaer GW. Role of neuregulin-1/ErbB signaling in cardiovascular physiology and disease: implications for therapy of heart failure. *Circulation* 2007;116:954–60.
2. Melenhorst WB, Mulder GM, Xi Q, Hoenderop JG, Kimura K, Eguchi S, van Goor H. Epidermal growth factor receptor signaling in the kidney: key roles in physiology and disease. *Hypertension* 2008;52:987–93.
3. Mei L, Xiong WC. Neuregulin 1 in neural development, synaptic plasticity and schizophrenia. *Nat Rev Neurosci* 2008;9:437–52.
4. Falls DL. Neuregulins: functions, forms, and signaling strategies. *Exp Cell Res* 2003;284:14–30.
5. Rio C, Rieff HI, Qi P, Khurana TS, Corfas G. Neuregulin and erbB receptors play a critical role in neuronal migration. *Neuron* 1997;19:39–50.
6. Gerecke KM, Wyss JM, Karavanova I, Buonanno A, Carroll SL. ErbB transmembrane tyrosine kinase receptors are differentially expressed throughout the adult rat central nervous system. *J Comp Neurol* 2001;433:86–100.
7. Thompson M, Lauderdale S, Webster MJ, Chong VZ, McClintock B, Saunders R, Weickert CS. Widespread expression of ErbB2, ErbB3 and ErbB4 in non-human primate brain. *Brain Res* 2007;1139:95–109.
8. Fox IJ, Kornblum HI. Developmental profile of ErbB receptors in murine central nervous system: implications for functional interactions. *J Neurosci Res* 2005;79:584–97.
9. Guyenet PG. The sympathetic control of blood pressure. *Nat Rev Neurosci* 2006;7:335–46.
10. Guyenet PG, Schreihofer AM, Stornetta RL. Regulation of sympathetic tone and arterial pressure by the rostral ventrolateral medulla after depletion of C1 cells in rats. *Ann N Y Acad Sci* 2001;940:259–69.
11. Matsukawa R, Hirooka Y, Nishihara M, Ito K, Sunagawa K. Neuregulin-1/ErbB signaling in rostral ventrolateral medulla is involved in blood pressure regulation as an antihypertensive system. *J Hypertens* 2011;29:1735–42.
12. Hirooka Y, Kishi T, Sakai K, Takeshita A, Sunagawa K. Imbalance of central nitric oxide and reactive oxygen species in the regulation of sympathetic activity and neural mechanisms of hypertension. *Am J Physiol Regul Integr Comp Physiol* 2011;300:R818–26.
13. Matsumura K, Abe I, Tsuchihashi T, Fujishima M. Central nitric oxide attenuates the baroreceptor reflex in conscious rabbits. *Am J Physiol* 1998;274:R1142–9.
14. Kagiyama S, Tsuchihashi T, Abe I, Fujishima M. Enhanced depressor response to nitric oxide in the rostral ventrolateral medulla of spontaneously hypertensive rats. *Hypertension* 1998;31:1030–34.
15. Garthwaite J. Concepts of neural nitric oxide-mediated transmission. *Eur J Neurosci* 2008;27:2783–2802.
16. Kishi T, Hirooka Y, Sakai K, Shigematsu H, Shimokawa H, Takeshita A. Overexpression of eNOS in the RVLM causes hypotension and bradycardia via GABA release. *Hypertension* 2001;38:896–901.
17. Kishi T, Hirooka Y, Ito K, Sakai K, Shimokawa H, Takeshita A. Cardiovascular effects of overexpression of endothelial nitric oxide synthase in the rostral ventrolateral medulla in stroke-prone spontaneously hypertensive rats. *Hypertension* 2002;39:264–68.
18. Kishi T, Hirooka Y, Kimura Y, Sakai K, Ito K, Shimokawa H, Takeshita A. Overexpression of eNOS in RVLM improves impaired baroreflex control of heart rate in SHRSP. Rostral ventrolateral medulla. Stroke-prone spontaneously hypertensive rats. *Hypertension* 2003;41:255–60.
19. Krainock R, Murphy S. Heregulin upregulates the expression of nitric oxide synthase (NOS)-1 in rat cerebellar granule neurons via the ErbB4 receptor. *J Neurochem* 2001;76:312–15.
20. Lemmens K, Fransen P, Sys SU, Brutsaert DL, De Keulenaer GW. Neuregulin-1 induces a negative inotropic effect in cardiac muscle: role of nitric oxide synthase. *Circulation* 2004;109:324–26.
21. Feron O, Zhao YY, Kelly RA. The ins and outs of caveolar signaling. m2 muscarinic cholinergic receptors and eNOS activation versus neuregulin and ErbB4 signaling in cardiac myocytes. *Ann N Y Acad Sci* 1999;874:11–19.
22. Sakai K, Hirooka Y, Matsuo I, Eshima K, Shigematsu H, Shimokawa H, Takeshita A. Overexpression of eNOS in NTS causes hypotension and bradycardia in vivo. *Hypertension* 2000;36:1023–28.
23. Chaudhury AR, Gerecke KM, Wyss JM, Morgan DG, Gordon MN, Carroll SL. Neuregulin-1 and erbB4 immunoreactivity is associated with neuritic plaques in Alzheimer disease brain and in a transgenic model of Alzheimer disease. *J Neuropathol Exp Neurol* 2003;62:42–54.
24. Eshima K, Hirooka Y, Shigematsu H, Matsuo I, Koike G, Sakai K, Takeshita A. Angiotensin in the nucleus tractus solitarii contributes to neurogenic hypertension caused by chronic nitric oxide synthase inhibition. *Hypertension* 2000;36:259–63.
25. Katoh M, Egashira K, Usui M, Ichiki T, Tomita H, Shimokawa H, Rakugi H, Takeshita A. Cardiac angiotensin II receptors are upregulated by long-term inhibition of nitric oxide synthesis in rats. *Circ Res* 1998;83:743–51.
26. Grazette LP, Boecker W, Matsui T, Semigran M, Force TL, Hajjar RJ, Rosenzweig A. Inhibition of ErbB2 causes mitochondrial dysfunction in cardiomyocytes: implications for herceptin-induced cardiomyopathy. *J Am Coll Cardiol* 2004;44:2231–38.
27. Minakuchi Y, Takeshita F, Kosaka N, Sasaki H, Yamamoto Y, Kouno M, Honma K, Nagahara S, Hanai K, Sano A, Kato T, Terada M, Ochiya T. Atelocollagen-mediated synthetic small interfering RNA delivery for effective gene silencing in vitro and in vivo. *Nucleic Acids Res* 2004;32:e109.
28. Kishi T, Hirooka Y, Kimura Y, Ito K, Shimokawa H, Takeshita A. Increased reactive oxygen species in rostral ventrolateral medulla contribute to neural mechanisms of hypertension in stroke-prone spontaneously hypertensive rats. *Circulation* 2004;109:2357–62.
29. Hirooka Y, Polson JW, Dampney RA. Pressor and sympathoexcitatory effects of nitric oxide in the rostral ventrolateral medulla. *J Hypertens* 1996;14:1317–24.
30. Iadecola C, Xu X, Zhang F, Hu J, el-Fakahany EE. Prolonged inhibition of brain nitric oxide synthase by short-term systemic administration of nitro-L-arginine methyl ester. *Neurochem Res* 1994;19:501–05.
31. Murillo H, Schmidt LJ, Tindall DJ. Tyrphostin AG825 triggers p38 mitogen-activated protein kinase-dependent apoptosis in androgen-independent prostate cancer cells C4 and C4-2. *Cancer Res* 2001;61:7408–12.
32. Tsai CM, Levitzki A, Wu LH, Chang KT, Cheng CC, Gazit A, Perng RP. Enhancement of chemosensitivity by tyrphostin AG825 in high-p185(neu) expressing non-small cell lung cancer cells. *Cancer Res* 1996;56:1068–74.
33. Li DP, Chen SR, Finnegan TF, Pan HL. Signalling pathway of nitric oxide in synaptic GABA release in the rat paraventricular nucleus. *J Physiol* 2004;554:100–10.
34. Woo RS, Li XM, Tao Y, Carpenter-Hyland E, Huang YZ, Weber J, Neiswender H, Dong XP, Wu J, Gassmann M, Lai C, Xiong WC, Gao TM, Mei L. Neuregulin-1 enhances depolarization-induced GABA release. *Neuron* 2007;54:599–610.
35. Chan SH, Wang LL, Wang SH, Chan JY. Differential cardiovascular responses to blockade of nNOS or iNOS in rostral ventrolateral medulla of the rat. *Br J Pharmacol* 2001;133:606–14.
36. Kimura Y, Hirooka Y, Sagara Y, Ito K, Kishi T, Shimokawa H, Takeshita A, Sunagawa K. Overexpression of inducible nitric oxide synthase in rostral ventrolateral medulla causes hypertension and sympathoexcitation via an increase in oxidative stress. *Circ Res* 2005;96:252–60.

Hypertension Research (2013), 1–7

www.nature.com/hr

ORIGINAL ARTICLE

Role of hypothalamic angiotensin type 1 receptors in pressure overload-induced mineralocorticoid receptor activation and salt-induced sympathoexcitation

Koji Ito[1], Yoshitaka Hirooka[2], Masatsugu Nakano[1], Nobuhiro Honda[1], Ryuichi Matsukawa[1] and Kenji Sunagawa[1]

Pressure overload enhances salt-induced sympathoexcitation through hypothalamic mineralocorticoid receptor (MR)-epithelial Na channel activation. Pressure overload also increases hypothalamic angiotensin type 1 receptors (AT1R). However, the role of AT1R in pressure overload-induced MR activation and salt-induced sympathoexcitation remains unknown. Therefore, the aim of the present study was to address this question. We performed aortic banding (AB) on mice from the Institute of Cancer Research. The expression of hypothalamic MR, serum/glucocorticoid-induced protein kinase-1 (SGK-1) and AT1R increased independently of plasma renin activity at 2 or 4 weeks after AB. Next, we performed AB in AT1aR-knockout (KO) mice and c57BL6/J wild-type (WT) mice. Sham-operated (Sham) mice were used as a control. Four weeks after AB (AB-KO or AB-WT), the expression of hypothalamic MR and SGK-1 increased in both AB-WT and AB-KO compared with Sham-WT and Sham-KO, respectively. The expression of AT1R was also greater in AB-WT than in Sham-WT. In addition, mice were fed a high-salt (8%) diet for an additional 4 weeks (ABH-KO and ABH-WT). High salt loading increased the urinary excretion of norepinephrine, a marker of sympathetic activity in ABH-WT, concomitant with hypothalamic MR activation, but not in ABH-KO. These results indicate that pressure overload activated hypothalamic MR independently of AT1R. After salt intake, however, AT1R was necessary to maintain hypothalamic MR activation and salt-induced sympathoexcitation.
Hypertension Research advance online publication, 31 January 2013; doi:10.1038/hr.2012.221

Keywords: angiotensin type 1 receptors; mineralocorticoid receptors; pressure overload; salt; sympathetic nervous system

INTRODUCTION

High salt intake causes sympathoexcitation and blood pressure elevation, particularly in salt-sensitive models.[1,2] It is well known that the central nervous system has an important role in salt-induced sympathoexcitation and hypertension.[3–5] Intracerebroventricular infusion of high-Na artificial CSF enhances sympathetic activity and increases blood pressure in both the salt-sensitive and salt-resistant models. The degree of increase, however, is greater in the salt-sensitive models than in the salt-resistant models.[6] In addition, we confirmed that there was also a greater blood pressure elevation in response to high-Na intracarotid artery infusion in the salt-sensitive model than in the salt-resistant model.[7] Therefore, an inappropriate response to high Na levels in the brain is suggested to be a key factor in salt-sensitive hypertension.

We recently reported that mice with pressure overload acquired salt sensitivity for sympathetic activity.[8] In mice with pressure overload, but not in Sham mice, high salt intake causes sympathoexcitation. Intracerebroventricular infusion of high-Na artificial CSF causes sympathoexcitation both in mice with pressure overload and in Sham mice. However, the degree of induction of sympathetic nerve activation is greater in mice with pressure overload than in Sham mice. We also confirmed an increased Na concentration in the brains of mice with pressure overload after salt intake.[8] These results suggest that in mice with pressure overload, the responses of sympathetic nerve activation to high Na levels in the brain is enhanced inappropriately. Furthermore, we confirmed that in mice with pressure overload, the hypothalamic mineralocorticoid receptor (MR)-epithelial Na channel (ENaC) pathway contributes to the acquisition of salt sensitivity for sympathetic activity.[9] In this model, the expression levels of hypothalamic angiotensin type 1 receptors (AT1R) also increased. Brain AT1R is known to be involved in sympathoexcitation in animal models of hypertension and heart failure.[10–13] However, the role of hypothalamic AT1R in pressure overload-induced MR activation and salt-induced sympathoexcitation remains unknown. Therefore, the aim of the present study was to answer this question. To this end, we performed aortic banding (AB)

[1]Department of Cardiovascular Medicine, Kyushu University Graduate School of Medical Sciences, Fukuoka, Japan and [2]Department of Advanced Cardiovascular Regulation and Therapeutics, Kyushu University Graduate School of Medical Sciences, Fukuoka, Japan
Correspondence: Dr K Ito or Dr Y Hirooka, Cardiovascular Medicine, Kyushu University Graduate School of Medical Sciences, 3-1-1, Maidashi, Higashi-ku, Fukuoka 812-8582, Japan.
E-mail: kojiitoh@cardiol.med.kyushu-u.ac.jp or hyoshi@cardiol.med.kyushu-u.ac.jp
Received 22 August 2012; revised 14 November 2012; accepted 23 November 2012

to create a pressure overload model using Institute of Cancer Research (ICR) or AT1aR-knockout (KO) mice and measured the plasma renin activity (PRA), plasma aldosterone concentration (PAC), sympathetic activity by urinary norepinephrine (uNE) excretion in response to a high-salt diet, MR expression, serum/glucocorticoid-induced protein kinase-1 (SGK-1, a marker of MR activity) expression, ENaC expression and AT1R expression in the hypothalamus.

METHODS

Animals

The study protocol was reviewed and approved by the Committee on Ethics of Animal Experiments, Kyushu University Graduate School of Medical Sciences, and conducted according to the Guidelines for Animal Experiments of Kyushu University and the Guide for the Care and Use of Laboratory Animals published by the US National Institute of Health (NIH publication No. 85-23, revised 1996). Ten-week-old male ICR mice (SLC, Hamamatsu, Japan), AT1aR KO mice (Jackson Laboratory, Bar Harbor, ME, USA; B6.$_{129}$P$_2$-*Agtr1a*^{tm1Unc}/J), and C57 black6/J (WT mice; SLC) were used.

Mouse pressure overload model preparation

The suprarenal abdominal aorta was banded in mice (AB mice) under sodium pentobarbital (25–35 mg kg^{-1} intraperitoneally anesthesia, and the depth of anesthesia was maintained by isoflurane inhalation (1.5–2.0%). The abdominal aorta was constricted at the suprarenal level with 5-0 silk sutures guided by a blunted 27-gauge needle, which was withdrawn as quickly as possible.[10,11] In the case of ICR mice, the mice were assigned 2 or 4 weeks later as AB2 or AB4 mice, and Sham mice served as control (Sham2 mice or Sham4 mice, respectively). In the case of the KO/WT mice, the mice were classified 4 weeks later as AB-KO mice or AB-WT mice, and Sham mice served as the control (Sham-KO or Sham-WT). Furthermore, the AB-KO mice, AB-WT mice and Sham-WT mice were fed with a high-salt (8% NaCl) diet for an additional 4 weeks (ABH-KO mice, ABH-WT mice, and ShamH-WT mice).

Evaluation of left ventricle systolic function

The left ventricle (LV) systolic function was evaluated by echocardiography. Serial M-mode echocardiography was performed on mice under light sodium pentobarbital anesthesia with spontaneous respiration. We used an echocardiography system (SSD5000; Aloka, Tokyo, Japan) with a dynamically focused 10-MHz linear array transducer. M-mode tracings were recorded from the short-axis view at the level of the papillary muscle. The LV end-diastolic diameter (LVDD), LV end-systolic diameter (LVSD) and LV wall thickness (LVWT) were measured. The LVWT was calculated as the mean thickness of the interventricular septum and the posterior LV wall. The per cent fractional shortening (%FS) was calculated as follows: %FS = (LVDD − LVSD)/LVDD × 100.

Measurement of PRA and PAC

To measure PRA and PAC, within minutes after the mice were injected with an overdose of sodium pentobarbital, a blood sample was collected from the right ventricle into a standard EDTA-containing syringe. The plasma obtained by centrifugation for 10 min at 6000 r.p.m. was used for the PRA and PAC measurements. PRA was measured by radioimmunoassay using a kit for animal samples (SRL Inc., Tokyo, Japan), and PAC was measured using an enzyme-linked immunosorbent assay.

Evaluation of sympathetic activity and confirmation of salt sensitivity

Sympathetic activity was evaluated by measuring 24-hour uNE excretion using high-performance liquid chromatography (SRL Inc.).[8,9]

The AB2, AB4, Sham2 and Sham4 mice were fed a high-salt diet (8%) or a regular-salt diet for 5 days. Sympathetic activity in response to a 5-day high-salt diet was evaluated by 24-hour uNE excretion to confirm the acquired salt sensitivity.

Measurement of blood pressure and heart rate

Under isoflurane anesthesia (1.5–2.0%), a catheter (stretched PE50 tubing) was inserted into the right carotid artery. PE50 tubing was tunneled subcutaneously from the neck incision to the back of the neck. PE50 tubing was filled with heparinized saline.

After the animals recovered from anesthesia (almost 3 h after surgical procedure), their conscious-state blood pressure and heart rate were measured.

Measurement of organ weight

After completion of the experiments, the mice were killed with an overdose of sodium pentobarbital, and the heart and lungs were removed and weighed.

Western blot analysis

The animals were killed with an overdose of sodium pentobarbital, and the hypothalamus, including circumventricular tissues, was obtained. The tissues were homogenized in a lysing buffer containing 40 mmol l^{-1} 4-(2-hydroxyethyl)-1-piperazineethanesulfonic acid, 1% Triton X-100, 10% glycerol, 1 mmol l^{-1} sodium orthovanadate and 1 mmol l^{-1} phenylmethylsulfonyl fluoride. The protein concentration was determined using a bicinchoninic acid protein assay kit (Pierce Chemical Co., Rockford, IL, USA). A 15-μg aliquot of protein from each sample was separated on a polyacrylamide gel with 10% sodium dodecyl sulfate. The proteins were subsequently transferred onto polyvinylidene difluoride membranes (Immobilon-P membranes; Millipore, Billerica, MA, USA). The membranes were incubated in immunoreaction enhancer solution (Can Get Signal; Toyobo, Osaka, Japan) with a rabbit immunoglobulin G polyclonal antibody against MR (1:1000; Santa Cruz Biotechnology, Santa Cruz, CA, USA), a rabbit polyclonal antibody against SGK-1 (1:1000; Abcam, Cambridge, UK), a rabbit immunoglobulin G monoclonal antibody against AT1R (1:1000; Santa Cruz Biotechnology), a goat immunoglobulin G polyclonal antibody against αENaC, a rabbit polyclonal antibody against βENaC or a rabbit polyclonal antibody against γENaC (1:1000; Santa Cruz Biotechnology). The membranes were then incubated with a horseradish peroxidase-conjugated horse anti-rabbit or anti-goat immunoglobulin G antibody (1:10 000). Glyceraldehyde 3-phosphate dehydrogenase was used as an internal control for the brain tissues. Immunoreactivity was detected by enhanced chemiluminescence autoradiography (ECL Western Blotting Detection Kit; Amersham Pharmacia Biotech, Uppsala, Sweden), and the positive bands on the film were analyzed using the public domain software NIH Image (developed at the US National Institutes of Health and available on the internet at http://rsb.info.nih.gov/nih-image/).

Statistical analysis

All values are expressed as the mean ± s.e. An analysis of variance was used to compare uNE excretion, organ weight, LVDD, LVWT, %FS and protein expression levels between groups. Any two mean values were compared by application of the Bonferroni procedure. Differences were considered significant when the *P*-value was <0.05.

RESULTS

Acquired salt sensitivity for sympathetic activity in AB mice

The sympathetic activity, as evaluated by uNE excretion in response to the 5-day high-salt diet, was increased in AB2 and AB4 mice but not in Sham2 and Sham4 mice (Figure 1). The sympathetic activity did not change in the groups without a high-salt diet.

PRA and PAC in AB2 and AB4 mice

Neither PRA nor PAC in the AB2 and AB4 mice differed from those of the nontreated control mice (Figure 2a).

Blood pressure and heart rate in AB2 and AB4 mice

The mean blood pressure was greater in the AB mice than in the Sham mice both 2 and 4 weeks after AB. The mean blood pressure in the AB4 mice was greater than that in the AB2 mice (Table 1).

Expression levels of hypothalamic MR, SGK-1, ENaC and AT1R in AB2 and AB4 mice

The expression levels of hypothalamic MR, SGK-1, αENaC and AT1R were greater in the AB2 and AB4 mice than in the Sham2 and Sham4 mice (Figure 2b). The expressions of hypothalamic βENaC and γENaC did not differ between the groups.

Characteristics of AB-KO and AB-WT mice

The body weight, relative heart weight and relative lung weight in the AB mice did not differ from those in the Sham mice (both WT and KO) (Figure 3a). Echocardiography revealed that LVWT was greater in the AB-WT and AB-KO mice than in the Sham-WT and Sham-KO mice. The %FS did not differ between the Sham mice and the AB mice (both WT and KO) (Figure 3b). Additionally, the sympathetic activity (measured by uNE excretion) did not differ between the Sham mice and the AB mice (both WT and KO) (Figure 3c).

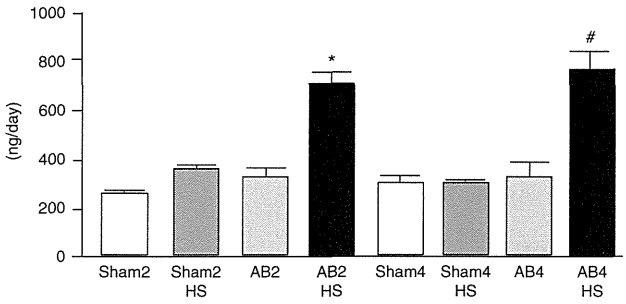

Figure 1 Urinary norepinephrine excretion in response to a 5-day high-salt diet in each group. HS indicates high-salt diet (*$P<0.05$ *vs.* Sham2, Sham2 + HS, and AB2, $n=6$–8, #$P<0.05$ *vs.* Sham4, Sham4 + HS, and AB4, $n=6$ for each). Sham2, 2 weeks after sham operation; Sham4, 4 weeks after sham operation; AB2, 2 weeks after aortic banding; AB4, 4 weeks after aortic banding.

Characteristics of ABH-KO and ABH-WT mice

The body weight and relative lung weight in the ABH mice were similar to those in the other groups in both the WT and KO mice. Compared with the AB and Sham mice, the relative heart weight in the ABH mice increased in both the WT and KO mice (Figure 3a). Echocardiography revealed that the LVWT was greater in the ABH-WT and ABH-KO mice than in the AB-WT and AB-KO mice, respectively. The %FS decreased in both the ABH-WT and ABH-KO mice compared with AB-WT and AB-KO mice, respectively. However, the extent to which %FS decreased was greater in the ABH-WT mice than in the ABH-KO mice (Figure 3b). In the WT mice, sympathetic activity (measured by uNE excretion) increased in the ABH mice compared with the AB or Sham mice but not the KO mice. Sympathetic activity in the ShamH-WT mice was higher than that in the sham-WT mice but lower than that in the ABH-WT mice (Figure 3c).

Blood pressure and heart rate in AB and ABH mice

The mean blood pressure increased in the AB-WT mice compared with that of the Sham-WT mice, and in the ABH-WT mice, the mean blood pressure was reduced to levels similar to that of the Sham-WT mice. The heart rate tended to increase in the AB-WT

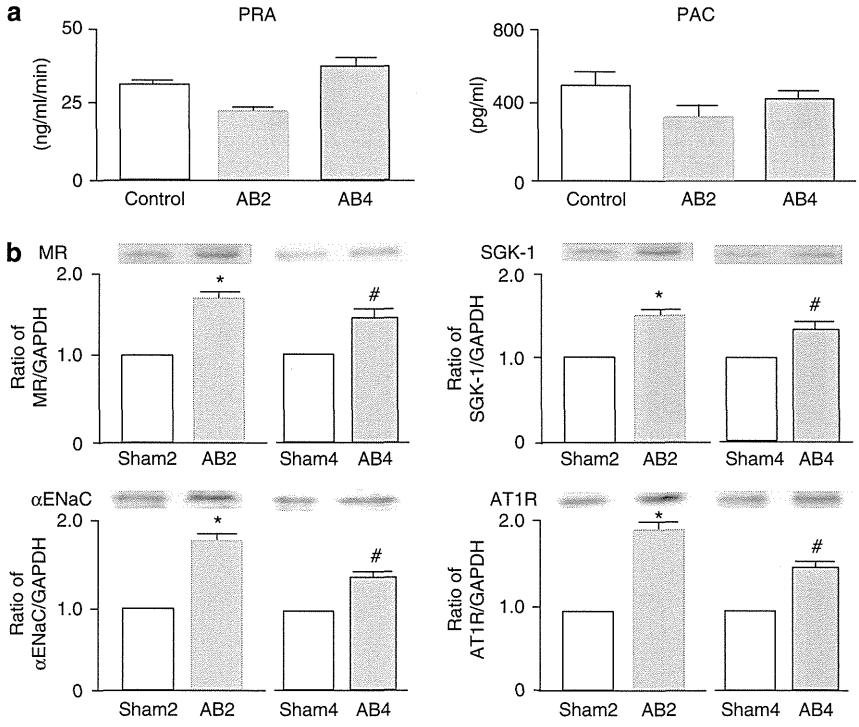

Figure 2 (**a**) PRA and PAC in AB2 and AB4 mice. Control indicates nontreated 10-week-old ICR mice. $n=5$ for each. PAC, plasma aldosterone concentration; PRA, plasma renin activity. (**b**) Representative western blots showing hypothalamic MR, SGK-1, αENaC and AT1R expression from each group. The graph shows the means for the quantification of four or five separate experiments. The data are the ratio relative to glyceraldehyde 3-phosphate dehydrogenase expression and are expressed as a ratio relative to Sham2 or Sham4, which were assigned a value of 1. (*$P<0.05$ *vs.* Sham2, #$P<0.05$ *vs.* Sham4.) AB2, 2 weeks after aortic banding; AB4, 4 weeks after aortic banding; Sham2, 2 weeks after sham operation; Sham4, 4 weeks after sham operation.

mice; a significant increase was observed in the ABH-WT mice compared with the Sham-WT mice (Table 1).

PAC in AB and ABH mice

In the WT mice, PAC significantly decreased in the ABH mice compared with the Sham or AB mice (Sham-WT, $443 \pm 79\,pg\,ml^{-1}$; AB-WT, $410 \pm 68\,pg\,ml^{-1}$; ABH-WT, $273 \pm 81\,pg\,ml^{-1}$, $n=5$ for each). In the KO mice, PAC also decreased in the ABH mice compared with the Sham or AB mice (Sham-WT, $569 \pm 33\,pg\,ml^{-1}$; AB-WT, $517 \pm 66\,pg\,ml^{-1}$; ABH-WT, $340 \pm 67\,pg\,ml^{-1}$, $n=5$ for each).

Table 1 Mean blood pressure and heart rate in each group

ICR	*Sham2*	*AB2*	*Sham4*	*AB4*
MBP (mm Hg)	96.9±1.8	126.4±4.3*	97.2±2.1	139.7±4.2#
HR (bpm)	495±9	510±14	514±19	529±10
c57BL6/J	*Sham*	*AB*	*ABH*	
MBP (mm Hg)	104.4±6.5	134.0±4.5[a]	96.5±3.0[b]	
HR (bpm)	506±16	530±30	546±12[a]	

*$P<0.05$ *vs.* Sham2, #$P<0.05$ *vs.* Sham4.
Abbreviations: AB, 4 weeks after aortic banding; ABH, AB mice with high salt diet for an additional 4 weeks; AB2, 2 weeks after aortic banding; AB4, 4 weeks after aortic banding; HR, heart rate; MBP, mean blood pressure; Sham2, 2 weeks after sham operation; Sham4, 4 weeks after sham operation.
[a]$P<0.05$ *vs.* Sham.
[b]$P<0.05$ *vs.* AB.

Expressions of hypothalamic MR, SGK-1, ENaC and AT1R

In the WT mice, the expression of hypothalamic MR, SGK-1 and αENaC were greater in the AB mice than in the Sham mice, and the expression of AT1R also increased in the AB mice compared with that in the Sham mice (Figure 4). In the KO mice, the expression levels of hypothalamic MR and SGK-1 also increased in the AB mice compared with that in the Sham mice (Figure 4). The extent to which the expression of SGK-1 increased in the WT mice, however, was greater than that of the KO mice (1.38 ± 0.06 *vs.* 1.21 ± 0.02, $P<0.05$, relative to Sham-WT or Sham-KO, respectively, which was assigned a value of 1). The enhanced expression levels of hypothalamic MR, SGK-1, αENaC and AT1R were maintained after high salt loading in the WT mice (ABH-WT). However, the expression of those proteins after high salt loading in KO mice (ABH-KO) returned to levels equal to that of the Sham mice (Figure 4). High salt loading did not alter the protein expression in WT mice (ShamH-WT) (MR, 0.96 ± 0.09; SGK1, 0.98 ± 0.08; αENaC, 0.94 ± 0.11, $N=3$ for each, relative to Sham-WT, which was assigned a value of 1), and the expression levels of hypothalamic βENaC and γENaC did not differ among the groups.

DISCUSSION

Our findings indicate that mice with pressure overload experienced increased hypothalamic MR activity that was independent of AT1R, and, after salt intake, AT1R is necessary to maintain brain MR activation and salt-induced sympathoexcitation. Thus, we suggest new targets for the studies of the prevention of salt-induced

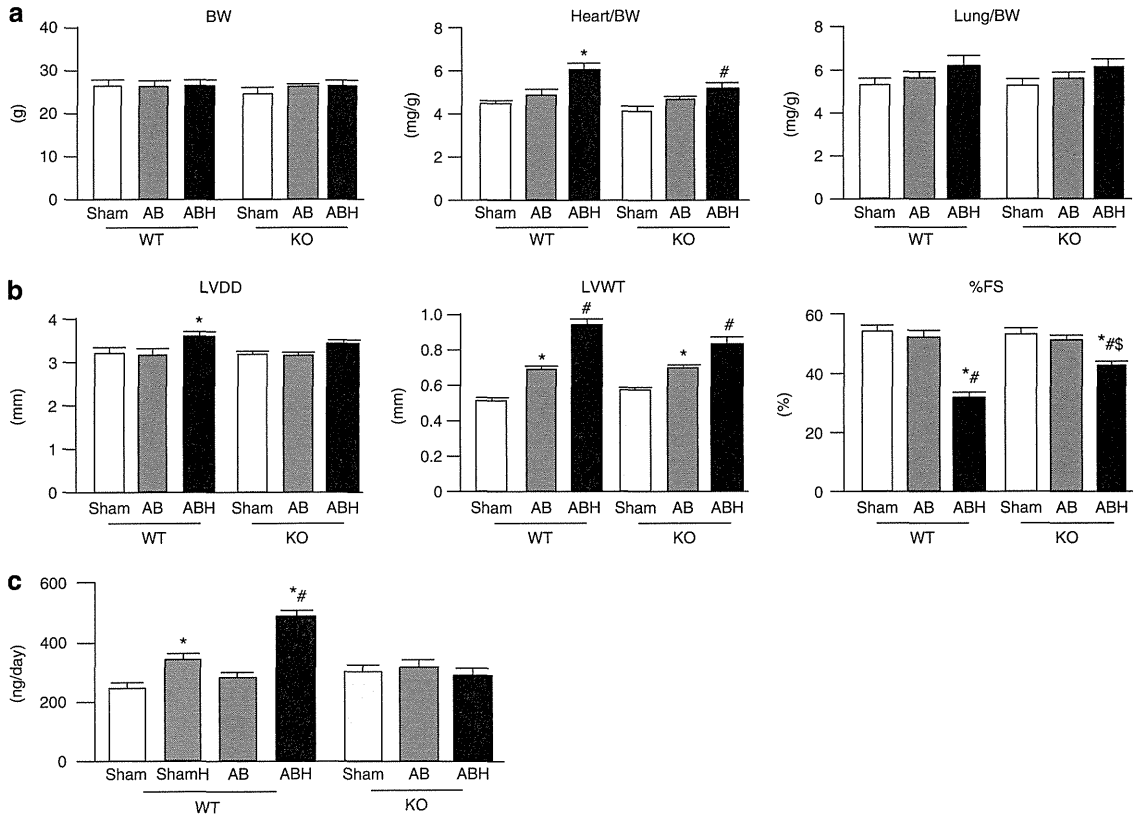

Figure 3 (**a**) BW, heart weight/BW and lung weight/BW in each group ($n=6$ in WT, $n=5$ in KO, *$P<0.05$ *vs.* Sham-WT, #$P<0.05$ *vs.* Sham-KO). BW, body weight. (**b**) Cardiac function in each group. LVDD, left-ventricular end-diastolic diameter; LVWT, LV wall thickness; %FS, percent fractional shortening ($n=5$ for each, *$P<0.05$ *vs.* Sham-WT or KO, #$P<0.05$ *vs.* AB-WT or KO, $P<0.05$ *vs.* ABH-WT). (**c**) Urinary norepinephrine excretion in each group ($n=8$ in WT, $n=5$ in KO, *$P<0.05$ *vs.* Sham-WT, #$P<0.05$ *vs.* others). AB, 4 weeks after aortic banding; ABH, AB mice with high salt diet for an additional 4 weeks; KO, AT1aR KO; Sham, sham-operated mice; WT, wild type c57black6/J mice.

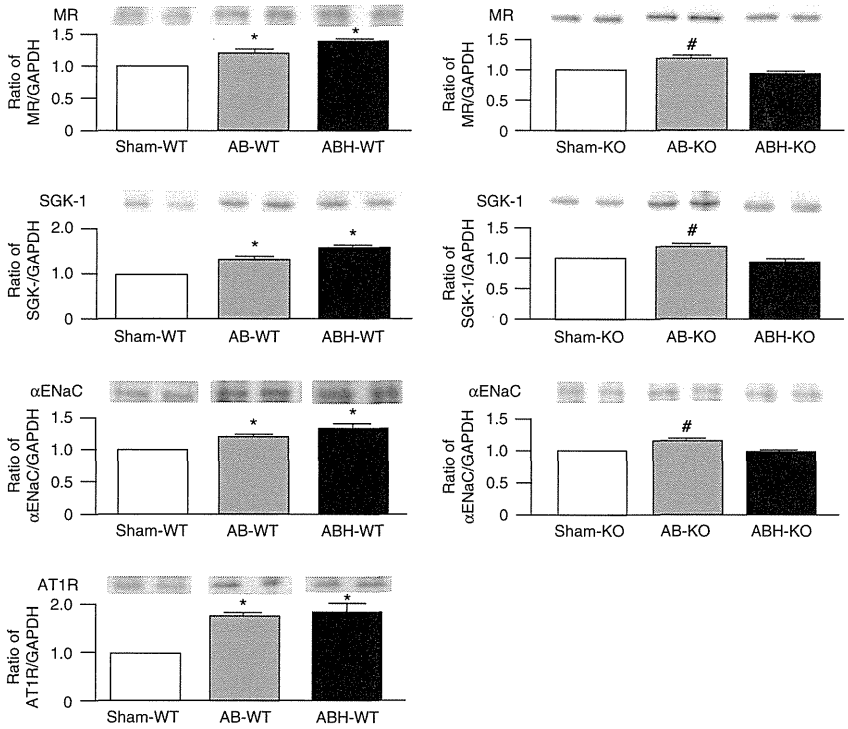

Figure 4 Representative western blots showing hypothalamic MR, SGK-1, αENaC and AT1R expression from each group. The graph shows the means for the quantification of five separate experiments in WT mice and three separate experiments in KO mice. The data are the ratio relative to glyceraldehyde 3-phosphate dehydrogenase expression and are expressed as a ratio relative to Sham-WT or Sham-KO, which were assigned a value of 1. ($^{*}P<0.05$ *vs.* Sham-WT, $^{\#}P<0.05$ *vs.* Sham-KO.) AB, 4 weeks after aortic banding; ABH, AB mice with high-salt diet for an additional 4 weeks; KO, AT1aR KO; Sham, sham-operated mice; WT, wild-type c57black6/J mice.

sympathoexcitation in patients with pressure overload conditions, such as hypertensive heart disease.

We previously demonstrated that pressure overload activated the hypothalamic MR-ENaC pathway; thus, concomitant salt loading led to sympathoexcitation.[8,9] We also found that pressure overload increased hypothalamic AT1R, and blockage of the brain AT1R effectively prevented salt-induced sympathoecitation.[8,9] However, the relationship between AT1R and MR and the role of these receptors in salt-induced sympathoexcitation remained unclear. We induced pressure overload by AB at the suprarenal level. It is possible that activation of the circulating renin-angiotensin system due to a decrease in renal blood flow might have influenced our observations in this study, because circulating renin-angiotensin system is known to affect brain renin-angiotensin system through circumventricular organs.[14] Therefore, we measured the PRA in mice with pressure overload. Both 2 and 4 weeks after AB, the PRA did not increase. In addition, we confirmed that the PAC in AB2 and AB4 mice was also at levels similar to that of the control group. On the other hand, the expressions of hypothalamic MR, SGK-1, αENaC and AT1R were greater in the AB2 and AB4 mice than in the Sham2 and Sham4 mice, respectively. These results indicate that activation of the hypothalamic MR pathway and increased AT1R do not depend on the PRA and PAC. Furthermore, we used AT1aR-KO mice in the present study. Pressure overload significantly increased hypothalamic MR and SGK-1 not only in WT mice but also in KO mice, although the degree of the pressure overload-induced increase in SGK-1 expression was greater in WT mice than in KO mice. These results indicate that the hypothalamic MR pathway is activated, at least in part, by pressure overload mechanisms that are independent of AT1aR.

Another important finding of the present study is that mice with pressure overload needed AT1aR to maintain hypothalamic MR activation after salt intake. The expression levels of hypothalamic MR, SGK-1, αENaC and AT1R were greater in the ABH-WT mice than in the Sham-WT mice, which is in agreement with sympathoexcitation. In contrast, the expression levels of hypothalamic MR, SGK-1 and αENaC in ABH-KO mice were at similar levels to those observed in the Sham-KO mice. Additionally, the sympathetic activity in the ABH-KO mice did not differ from that of the Sham-KO mice, suggesting that salt-induced sympathoexcitation in mice with pressure overload requires AT1aR.

We did not address the role of the AT1b receptor in AT1aR-KO mice in the present study. We previously confirmed that intracerebroventricular infusion of the AT1 receptor blocker failed to prevent pressure overload-induced hypothalamic MR enhancement.[9] In addition, salt-induced sympathoexcitation was completely blocked in the ABH-KO mice in the present study, suggesting the requirement of AT1aR in sympathoexcitation. Expression of the brain AT1b receptor is reported to occur at similar levels in WT mice and AT1aR-KO mice.[15] Based on these findings, we believe that AT1bR is not responsible for salt-induced sympathoexcitation.

The precise mechanism(s) involved in AT1R-independent hypothalamic MR activation remains unknown. Aldosterone is a major ligand of MR,[16] and it has been suggested that aldosterone is synthesized locally in the brain.[17,18] Hypothalamic aldosterone synthesis is reported to increase by high salt loading in a salt-sensitive hypertensive model. In the present study, pressure overload-induced hypothalamic MR activation was caused before high salt loading; therefore, aldosterone-independent mechanisms might contribute to

this mechanism. In the kidneys, small G protein Rac1 was demonstrated to activate the MR pathway in an aldosterone-independent manner.[19] Therefore, it is possible that a similar mechanism might be responsible for the pressure overload-induced hypothalamic MR activation that is independent of aldosterone.

The AT1R-dependent mechanism(s) involved in hypothalamic MR activation and sympathoexcitation after high salt loading also remains unclear. In both WT and KO mice, the PAC in ABH mice decreased compared with that of the Sham or AB mice. This finding suggested that the hypothalamic MR activation was independent of systemic aldosterone. In mice with pressure overload, high salt loading is presumed to increase the Na levels in the CSF,[8] which may increase brain aldosterone synthesis.[18] CYP11B2, an aldosterone synthase, is activated by angiotensin II via AT1R.[20] Therefore, in mice with pressure overload, high salt loading might lead to an increase in aldosterone synthesis via AT1R. Interestingly, the expression levels of hypothalamic MR-SGK-1-αENaC were lower in ABH-KO mice than in AB-KO mice but were at similar levels in Sham-KO mice. High salt loading is reported to decrease MR pathway activity.[21] Therefore, in the AT1aR-absent condition, the MR pathway-inactivated mechanisms might have a significant role in ABH-KO mice. However, we did not address these issues in the present study, and further studies are warranted to clarify the mechanisms.

We failed to demonstrate the attenuation of pressure overload-induced LV hypertrophy in AB-KO and ABH-KO mice. However, it has been reported that pressure overload induced LV hypertrophy in AT1aR-KO mice.[22] In the present study, we confirmed that aortic banding increased blood pressure in the WT mice. Although we did not measure blood pressure in the KO mice, the baseline blood pressure was ~20 mm Hg lower in AT1aR-KO mice than in WT mice.[22–24] However, the degree of blood pressure elevation due to aortic banding was similar to that observed in the WT mice,[22] and we successfully demonstrated LV hypertrophy in AB-KO mice, which suggests that the impact of aortic banding on LV hypertrophy is similar between WT mice and KO mice. In the present study, we started to feed the mice with a high-salt diet 4 weeks after AB (ABH mice). LV function was more deteriorated in the ABH mice than in the AB mice (both KO and WT). The blood pressure in the ABH-WT mice decreased to levels similar to or lower than those observed in the Sham-WT mice, which was most likely due to LV dysfunction.[8] The decrease in %FS was smaller in the ABH-KO mice than in the ABH-WT mice. The greater decreases in %FS in the ABH-WT mice than in the ABH-KO mice observed in the present study might have been caused by AT1R-mediated salt-induced sympathoexcitation.

In the present study, we evaluated three ENaC subunits (αENaC, βENaC and γENaC) and demonstrated that pressure overload increased the expression of hypothalamic αENaC. ENaC are reported to exist in the choroid plexus[25] and neurons of the hypothalamus and supraoptic nucleus.[26] In addition, a recent study reported that αENaC exists in both magnocellular neurons and parvocellular neurons, but βENaC and γENaC exist only in magnocellular neurons in the hypothalamus.[26] In addition, we recently demonstrated that three ENaC subunits also exist in the choroid plexus and contribute to salt-sensitive hypertensive mechanisms in stroke-prone spontaneously hypertensive rats.[7] As we performed western blotting using the hypothalamus including the circumventricular organs, we were not able to precisely determine the site of ENaC expression in the present study. Therefore, further studies are needed to clarify the site specificity and the pathophysiological significances of the enhanced expression of αENaC in mice with pressure overload.

Previously, in the case of ICR mice, we reported increased-αENaC expression in mice with pressure overload (AB mice). The expressions of γENaC, however, increased in mice with pressure overload after salt loading (ABH mice).[9] The reasons for these discrepancies remain unclear. The genetic backgrounds of the response for salt loading differ between ICR mice and c57black/J mice. In fact, c57black/J mice are known as a salt-sensitive model.[27] We also confirmed the salt-induced sympathoexcitation in ShamH-WT mice in the present study without changing the expression levels of hypothalamic MR-SGK-1-αENaC. Therefore, the differences in the genetic backgrounds between the two strains might affect the enhancement of the ENaC subunits in response to high salt loading.

In conclusion, the present findings strongly suggest that pressure overload activates hypothalamic MR independently of AT1R. After salt intake, however, AT1R is necessary to maintain hypothalamic MR activation and salt-induced sympathoexcitation.

CONFLICT OF INTEREST

The authors declare no conflict of interest.

ACKNOWLEDGEMENTS

We express our sincere thanks to Naomi Shirouzu for help with the western blot analysis. This work was supported by Grants-in-Aid for Scientific Research from the Japan Society for the Promotion Science (21790730, 24390198).

1 Wang JM, Veerasingham SJ, Tan J, Leenen FH. Effects of high salt intake on brain AT1 receptor densities in Dahl rats. *Am J Physiol Heart Circ Physiol* 2003; **285**: H1949–H1955.
2 Stocker SD, Madden CJ, Sved AF. Excess dietary salt intake alters the excitability of central sympathetic networks. *Physiol Behav* 2010; **100**: 519–524.
3 Huang BS, Van Vliet BN, Leenen FH. Increases in CSF[Na^+] precede the increases in blood pressure in Dahl S rats and SHR on high-salt diet. *Am J Physiol Heart Circ Physiol* 2004; **287**: H1160–H1166.
4 Blaustein MP, Leenen FH, Chen L, Golovina VA, Hamlyn JM, Pallone TP, Van Huysse JW, Zhang J, Wier WG. How NaCl raises blood pressure: a new paradigm for the pathogenesis of salt-dependent hypertension. *Am J Physiol Heart Circ Physiol* 2012; **302**: H1031–H1049.
5 Takahashi H, Yoshika M, Komiyama Y, Nishimura M. The central mechanism underlying hypertension: areview of the roles of sodium ions, epithelial sodium channels, the renin-angiotensin-aldosterone system, oxidative stress and endogenous digitalis in the brain. *Hypertens Res* 2011; **34**: 1147–1160.
6 Huang BS, Wang H, Leenen FH. Enhanced sympathoexcitatory and pressor responses to central Na^+ in Dahl salt-sensitive vs. -resistnat rats. *Am J Physiol Heart Circ Physiol* 2001; **281**: H1881–H1889.
7 Nakano M, Hirooka Y, Matsukawa R, Ito K, Sunagawa K. Mineralocorticoid receptors/epithelial Na^+ channels in the choroid plexus are involved in hypertensive mechanisms in stroke-prone spontaneously hypertensive rats. *Hypertens Res* (e-pub ahead of print 25 October 2012; doi:10.1038/hr.2012.174).
8 Ito K, Hirooka Y, Sunagawa K. Acquisition of brain Na sensitivity contributes to salt-induced sympathoexcitation and cardiac dysfunction in mice with pressure overload. *Circ Res* 2009; **104**: 1004–1011.
9 Ito K, Hirooka Y, Sunagawa K. Blockade of mineralocorticoid receptors improves salt-induced left-ventricular systolic dysfunction through attenuation of enhanced sympathetic drive in mice with pressure overload. *J Hypertens* 2010; **28**: 1449–1458.
10 Eshima K, Hirooka Y, Shigematsu H, Matsuo I, Koike G, Sakai K, Takeshita A. Angiotensin in the nucleus tractus solitarii contributes to neurogenic hypertension caused by chronic nitric oxide synthase inhibition. *Hypertension* 2000; **36**: 259–263.
11 Shigematsu H, Hirooka Y, Eshima K, Shihara M, Tagawa T, Takeshita A. Endogenous angiotensin II in the NTS contributes to sympathetic activation in rats with aortocaval shunt. *Am J Physiol Regul Integr Comp Physiol* 2001; **280**: R1665–R1673.
12 Allen AM. Role of angiotensin in the rostral ventrolateral medulla in the development and maintenance of hypertension. *Curr Opin Pharmacol* 2011; **11**: 117–123.
13 Wang WZ, Gao L, Wang HJ, Zucker IH, Wang W. Interaction between cardiac sympathetic afferent reflex and chemoreflex is mediated by the NTS AT1 receptors in heart failure. *Am J Physiol Heart Circ Physiol* 2008; **295**: H1216–H1226.
14 Hendel MD, Collister JP. Contribution of the subfornical organ to angiotensin II-induced hypertension. *Am J Physiol Heart Circ Physiol* 2005; **288**: H680–H685.
15 Rocha MJ, Chen Y, Oliveira GR, Morris M. Physiological regulation of brain angiotensin receptor mRNA in AT1a deficient mice. *Exp Neurol* 2005; **195**: 229–235.
16 Nagai Y, Miyata K, Sun GP, Rahman M, Kimura S, Miyatake A, Kiyomoto H, Kohno M, Abe Y, Yoshizumi M, Nishiyama A. Aldosterone stimulates collagen gene expression

and synthesis via activation of ERK1/2 in rat renal fibroblasts. *Hypertension* 2005; **46**: 1039–1045.
17 Gomez-Sanchez EP, Gomez-Sanches CM, Plonczynski M, Gomez-Sanchez CE. Aldosterone synthesis in the brain contributes to Dahl salt-sensitive rat hypertension. *Exp Physiol* 2009; **95**: 120–130.
18 Huang BS, White RA, Ahmad M, Jeng AY, Leenen FH. Central infusion of aldosterone synthase inhibitor prevents sympathetic hyperactivity and hypertension by central Na^+ in Wister rats. *Am J Physiol* 2008; **295**: R166–R172.
19 Shibata S, Nagase M, Yoshida S, Kawarazaki W, Kurihara H, Tanaka H, Miyoshi J, Takai Y, Fujita T. Modification of mineralocorticoid receptor function by Rac1 GTPase: implication in proteinuric kidney. *Nat Med* 2008; **14**: 1370–1376.
20 Lai L, Chen J, Hao CM, Lin S, Gu Y. Aldosterone promotes fibronectin production through a Smad2-dependent TGF-β1 pathway in mesangial cells. *Biochem Biophys Res Commun* 2006; **348**: 70–75.
21 Lienhard D, Lauterburg M, Escher G, Frey FJ, Frey BM. High salt intake down-regulates colonic mineralocorticoid receptors, epithelial sodium channels and 11 β-Hydroxysteroid dehydrogenase type 2. *PLoS One* 2012; **7**: e37898.
22 Harada K, Komuro I, Shiojima I, Hayashi D, Kudoh S, Mizuno T, Kijima K, Matsubara H, Sugaya T, Murakami K, Yazaki Y. Pressure overload induces cardiac hypertrophy in angiotensin II type 1A receptor knockout mice. *Circulation* 1998; **97**: 1952–1959.
23 Chen D, Greca LL, Head GA, Walther T, Mayorov DN. Blood pressure reactivity to emotional stress is reduced in AT1A-receptor knockout mice on normal, but not high salt intake. *Hypertens Res* 2009; **32**: 559–564.
24 Wichi RB, Farah V, Chen Y, Irigoyen MC, Morris M. Deficiency in angiotensin AT1a receptors prevents diabetes-induced hypertension. *Am J Physiol Regul Integr Comp Physiol* 2007; **292**: R1184–R1189.
25 Amin MS, Reza E, Wang H, Leenen FH. Sodium transport in the choroid plexus and salt-sensitive hypertension. *Hypertension* 2009; **54**: 860–867.
26 Teruyama R, Sakuraba M, Wilson LL, Wandrey NEJ, Armstrong WE. Epithelial Na^+ sodium channels in magnocellular cells of the rat supraoptic and paraventricular nuclei. *Am J Physiol Endocrinol Metab* 2012; **302**: E273–E285.
27 Escano CS, Armando I, Wang X, Asico LD, Pascua A, Yang Y, Wang Z, Lau YS, Jose PA. Renal dopaminergic defect in C57Bl/6J mice. *Am J Physiol Regul Integr Comp Physiol* 2009; **297**: R1660–R1669.

Circulation Journal
Official Journal of the Japanese Circulation Society
http://www.j-circ.or.jp

ORIGINAL ARTICLE
Arrhythmia/Electrophysiology

Gender Disparities in Quality of Life and Psychological Disturbance in Patients With Implantable Cardioverter-Defibrillators

Anita Rahmawati, MD; Akiko Chishaki, MD, PhD; Hiroyuki Sawatari, BSc; Miyuki Tsuchihashi-Makaya, PhD; Yuko Ohtsuka, BSc; Mori Nakai, MD, PhD; Mami Miyazono, PhD; Nobuko Hashiguchi, PhD; Harumizu Sakurada, MD, PhD; Masao Takemoto, MD, PhD; Yasushi Mukai, MD, PhD; Shujiro Inoue, MD, PhD; Kenji Sunagawa, MD, PhD; Hiroaki Chishaki, MD

Background: Implantable cardioverter-defibrillator (ICD) has improved prognosis in fatal arrhythmia and the number of ICD implantations has increased. ICD-related psychological problems and impaired quality of life (QOL), however, have been observed. This study examined whether gender differences exist in QOL and psychological disturbances in ICD patients.

Methods and Results: Consecutive outpatients (n=179; mean age, 60.5±15.9 years; 81% male) with ICD implantations completed questionnaires consisting of the Short Form-8 (SF-8), Beck Depression Inventory, Impact of Event Scale-Revised (IES-R), State-Trait Anxiety Inventory, and Worries about ICD. One-way multivariate analysis of variance (MANOVA) showed women to have impaired QOL on the role physical functioning ($F_{15,157}$=4.57, P<0.05) and bodily pain ($F_{15,157}$=5.26, P<0.05) subscales of the SF-8. More women reported depression ($F_{15,157}$=5.37, P<0.05) and worry about ICD than men ($F_{15,157}$=6.62, P<0.05). Moreover, women also had higher IES-R scores indicating post-traumatic stress disorder (PTSD) than men ($F_{15,157}$=5.87, P<0.05).

Conclusions: Women reported poorer QOL on 2 subscales: role physical functioning and bodily pain. There was a significant relationship between gender and depression, worry about ICD, and PTSD, but not for anxiety. Female patients need more psychological interventions following ICD implantation. (*Circ J* 2013; **77:** 1158–1165)

Key Words: Depression; Gender disparities; Implantable cardioverter-defibrillator; Post-traumatic stress disorder; Quality of life

Many studies have established that use of the implantable cardioverter-defibrillator (ICD) has resulted in improved survival in selected patients for primary and secondary prevention of sudden cardiac death (SCD).[1] Despite its life-saving benefit, experiencing ICD firings can be frightening and can affect the psychological dimensions. Nervousness, dizziness, weakness, and fear are the most common responses to ICD shock.[2] Approximately half of the patients with ICD implantation had depression or anxiety disorder[3] and vice versa: in hospitalized patients with depression there was a higher rate of ICD implantation on admission.[4] Restriction of quality of life (QOL) in patients receiving shocks was also identified in some previous studies.[5–7]

A prospective study has indicated that emotional distress is related to all-cause as well as cardiac-related mortality in patients with an ICD.[4,8,9] A study in Japanese patients with heart failure found that the QOL score could predict cardiac death independently of other prognostic factors.[10] The relationship between depression and mortality may be explained by the increased risk of arrhythmias and ICD shocks in patients with chronic levels of depression.[8,9] By the same token, catastrophic disaster, which can cause post-traumatic stress disorder (PTSD),

Received August 27, 2012; revised manuscript received October 30, 2012; accepted December 10, 2012; released online January 22, 2013 Time for primary review: 15 days

Department of Cardiovascular Medicine (A.R., M.T., Y.M., S.I., K.S.), Department of Health Sciences (A.C., H. Sawatari, M.M., N.H.), Kyushu University Graduate School of Medical Sciences, Fukuoka; Department of Healthcare Management, College of Healthcare Management, Fukuoka (H.C.); Department of Nursing, Kitasato University, Sagamihara (M.T.-M.); Department of Cardiology, Tokyo Metropolitan Hiroo Hospital, Tokyo (Y.O., M.N.); and Tokyo Metropolitan Health and Medical Treatment Corporation Ookubo Hospital, Tokyo (H. Sakurada), Japan

Mailing address: Akiko Chishaki, MD, PhD, Department of Health Sciences, Kyushu University Graduate School of Medical Sciences, 3-1-1 Maidashi, Higashi-ku, Fukuoka 812-8582, Japan. E-mail: chishaki@hs.med.kyushu-u.ac.jp

ISSN-1346-9843 doi:10.1253/circj.CJ-12-1116

Table 1. Patient Baseline Characteristics

	Female (n=34)	Male (n=145)	Total (n=179)	P-value
Demographics				
Age (years)	53.5±19.3	62.2±14.5	60.5±15.9	<0.01
Older age (≥65 years)	14 (41.2)	68 (46.9)	82 (45.8)	0.55
Smoking	3 (8.8)	65 (45.5)	68 (38.4)	<0.001
Clinical factors				
Indication (secondary prevention)	23 (67.6)	88 (60.7)	111 (62)	0.45
Prior history of heart failure	8 (23.5)	47 (32.4)	55 (30.7)	0.31
NYHA class III/IV	2 (10)	18 (24.7)	20 (21.5)	0.22
LVEF (%)	58.1 (19.1)	52.8 (18.5)	53.8 (18.7)	0.12
Inappropriate shocks	10±29.4	36±25	46±25.8	0.60
Presence of shock with syncope	3 (8.8)	16 (11.2)	19 (10.8)	1.00
Presence of shock without syncope	11 (32.3)	40 (28)	51 (29)	0.61
Ischemic etiology	6 (17.6)	54 (37.2)	60 (33.5)	0.03
Comorbidity				
Hypertension	12 (35.3)	67 (46.2)	79 (44.1)	0.25
Diabetes	6 (17.6)	29 (20.1)	35 (19.7)	0.74
Arrhythmia attack				0.52
Ventricular fibrillation	8 (26.7)	39 (32)	47 (30.9)	
Polymorphic ventricular tachycardia (pulseless)	4 (13.4)	8 (6.6)	12 (7.9)	
Sustained ventricular tachycardia (with deteriorated hemodynamics)	11 (36.7)	42 (34.4)	53 (34.9)	
Non-sustained ventricular tachycardia	6 (20)	20 (16.4)	26 (17.1)	
Syncope	1 (3.3)	13 (10.7)	14 (9.2)	

Data given as mean±SD or n (%).
LVEF, left ventricular ejection fraction; NYHA, New York Heart Association.

also has been reported to be associated with increased incidence of tachyarrhythmias.[11] Therefore, psychological symptoms that present in a proportion of ICD patients should not be underestimated.

There are significant sex differences in ICD implantation rates. Male subjects are increasingly more likely to undergo ICD implantation than female subjects for primary or secondary prevention, with this difference being more marked in the elderly.[12–14] The cause of this disparity is unclear, but potential explanations include differences in exercise tolerance, autonomic modulation, intrinsic properties of the sinus node, and higher prevalence of ischemic heart disease in men than in women.[13,15]

A previous study showed that physical functioning (PF) was worse in women than men and there was a high tendency of depression in women.[16] One systematic review noted various impacts of gender on QOL and psychological distress, although women seemed to have a higher prevalence of anxiety and tended to report poorer physical and mental health.[17] Furthermore, only with appropriate care, can female ICD patients return to previous levels of physical and psychological functioning.[18]

In the Asia-Pacific region, Japan has the largest number of ICD implants.[19] There are still limited studies, however, on gender differences in the response to ICD therapy in the Japanese population. One of the aims of the current study was to examine whether women were at a greater risk of increased anxiety; worry about ICD; depression; PTSD; and lower QOL. In addition, we tested the correlation between stress, anxiety components and depression, and QOL in men and women. The strength of gender differences as a predictor of QOL restriction and of psychological problems was also studied.

Methods

Subjects

Consecutive ICD patients who regularly visited the outpatient clinics at Kyushu University Hospital and Tokyo Metropolitan Hiroo Hospital from July 2005 to November 2008 were enrolled in this study. The total group consisted of 145 men and 34 women (mean age, 62.2±14.5 years vs. 53.5±19.3 years, respectively). Upon obtaining written informed consent, each ICD patient completed a set of questionnaires to assess QOL and psychological factors. This study was approved by the Ethics Committee of Kyushu University Graduate School of Medical Sciences and Tokyo Metropolitan Hiroo Hospital, and conducted in accordance with the Declaration of Helsinki.

Demographic variables consisted of gender, age, older age (≥65 years), and smoking. Clinical variables included indication of ICD implantation, prior history of heart failure, New York Heart Association (NYHA) class, left ventricular ejection fraction (LVEF) from echocardiography, presence of appropriate and inappropriate ICD shock, presence of ICD shocks with and without syncope, underlying heart disease (ischemic vs. non-ischemic, with non-ischemic defined as valvular heart disease, dilated cardiomyopathy, hypertrophic cardiomyopathy, long QT syndrome, Brugada syndrome, arrhythmogenic right ventricular dysplasia, cardiac sarcoidosis, and hypertensive heart disease), comorbidity (including hypertension, dyslipidemia, and diabetes), and arrhythmia attack before ICD implantation. Information on clinical variables was retrieved from the patients' medical records.

Patient characteristics for the total group are given in Table 1. Of 179 patients enrolled in the study, 111 patients (62%) had secondary prevention for SCD and 46 patients (25.8%) received

Table 2. Worries About Implantable Cardioverter-Defibrillator Scale

Items
1. It bothers me not knowing when the ICD will fire.
2. I worry about the ICD firing and creating a scene.
3. I am afraid of being alone if the ICD fires and I need help.
4. I worry about the ICD not firing sometime when I need it.
5. I worry that I need the ICD to keep my heart working right.
6. I can't stop thinking about the ICD.
7. I feel better knowing that I have the ICD in case I need it.
8. It bothers me that I have to see doctors so often for check-ups.
9. It bothers me that there is a "bump" where the ICD is.
10. It bothers me that I have to wear clothes that cover up the place where the ICD sticks out.
11. The feeling I get in my body when the ICD fires bothers me.
12. I feel itching on my ICD scar.
13. I feel pain on my ICD scar.
14. I worry that the ICD will fire when it's not supposed to.
15. I worry about how I will feel when the ICD fires.
16. I am nervous that if I exercise my heart might start beating faster and make the ICD fire.
17. I feel frustrated that I have to go into the hospital every couple of years to have the battery changed.
18. I worry that my medical bills will cost a lot of money.
19. I worry about not being able to get a job in future because of the ICD.
20. I feel my life better since I got the ICD.
21. It bothers me that I have to be careful around magnetic devices like the security system at the airport.
22. It bothers me that I am not supposed to drive a car in case the ICD fires.
23. I worry about traveling to a place where there aren't any doctors who know about the ICDs.
24. I worry that paramedics don't know how the ICD works.
25. I worry that my friends will find out I have an ICD.
26. I feel safer since I got my ICD.

Items 7, 20, and 26 are reversed-scored to reflect the opposite valence of these questions.
ICD, implantable cardioverter-defibrillator.

inappropriate ICD shocks. Ischemic etiology was a contributing factor in 60 patients (33.5%), and 20 patients (21.5%) had NYHA class III/IV.

Assessment of QOL and Psychological Factors

The following questionnaires were used to assess QOL, anxiety, depression, and PTSD symptoms. Measures included the Short Form-8 (SF-8), Japanese version of State-Trait Anxiety Inventory (STAI), Beck Depression Inventory (BDI), Impact of Event Scale-Revised (IES-R), and Worries about ICD (WAICD) Scale. The first 4 of these questionnaires have been linguistically validated. The WAICD was adapted from the Index of Subjective Concerns for People with ICDs (ISCP-ICD) and translated directly into Japanese.[5]

The SF-8 is a commonly used instrument of health-related QOL. It is based on extensive previous work with the SF-36 and SF-12 (Quality Metric, RI, USA) and consists of 8 subscales, each representing 1 health profile dimension: PF, role PF (RP), bodily pain (BP), general health perception, vitality, social functioning, role emotional functioning, and mental health. Each item is assessed using 5- or 6-point Likert scale, and is standardized according to the scoring system. This questionnaire yields summary scores for the physical (physical component summary, PCS) and mental (mental component summary, MCS) components of health-related QOL. Both summary scores are reported on a scale from 0 to 100, with higher scores indicating better physical and mental health.[19,20]

The BDI is the most frequently used self-report method of depression screening in general populations, and it also provides a measure of the severity of depression.[21,22] It consists of 21 multiple-choice questions and has high internal consistency. Depression severity is categorized as follows: absent, 0–12; mild, 13–19; moderate, 20–28; and severe, ≥29. These cut-off points were verified for the likelihood of detection of depressive symptoms in Japanese subjects.[22]

The IES-R is a 22-item scale rated from 0 (not at all) to 4 (extremely) with respect to distressing events during the past week. High internal consistency and high reproducibility have been reported for the Japanese translation of the IES-R.[23] We set the cut-off value for PTSD as 20 in accordance with a previous report.[24]

The STAI measures reported anxiety symptoms.[23] It measures state anxiety and trait anxiety. The range of scores is 20–80, higher scores indicating greater anxiety. State anxiety reflects how a patient generally feels at the time of the assessment. Trait anxiety is defined as a relatively enduring personality characteristic, or more specifically as anxiety proneness.[25] The cut-off values of 40 in men and 42 in women for trait anxiety have been used to dichotomize subjects into low and high-anxiety groups. Meanwhile, an STAI-state score >44 defines an individual as highly anxious.[23] Applying this cut-off level, we defined ICD patients with STAI-state scores ≤44 as low anxiety, and those with scores >44 as high anxiety.

The WAICD is a 26-item self-report measure designed to assess QOL issues associated with having an ICD implantation (Table 2). The items are measured on a 5-point Likert scale anchored at 1 end by "0, not at all true" and at the other end by "4, extremely true", reflecting the degree to which the

Table 3. QOL and Other Psychological Scores vs. Gender

	Female	Male	$F_{15,157}$
QOL			
Physical functioning	43±9.4	46.1±9.5	3.16
Role physical functioning	43.3±9.1	47.0±8.8	4.57*
Bodily pain	50.5±10.2	54.3±8.3	5.26*
General health	43.5±5	45.6±7.4	2.40
Vitality	48.9±7.1	51.8±8.4	3.90
Social functioning	48.6±7.6	49.3±8.8	0.03
Role emotional functioning	43.6±9.9	46.3±7.7	2.07
Mental health	47.3±9.6	49.3±8.8	1.46
PCS	44.3±8.8	48.7±9.0	6.50*
MCS	48.1±10.8	50.1±9.7	1.10
Anxiety	40.9±12.1	38.4±11	1.34
Depression	9.3±9.2	5.8±7.4	5.37*
PTSD	17.7±21.3	10.4±14.8	5.87*
WAICD	40.6±18.6	31.0±18.8	6.62*

*P<0.05. Data given as mean±SD.
MCS, mental component summary; PCS, physical component summary; PTSD, post-traumatic stress disorder; QOL, quality of life; WAICD, Worries About Implantable Cardioverter-Defibrillator.

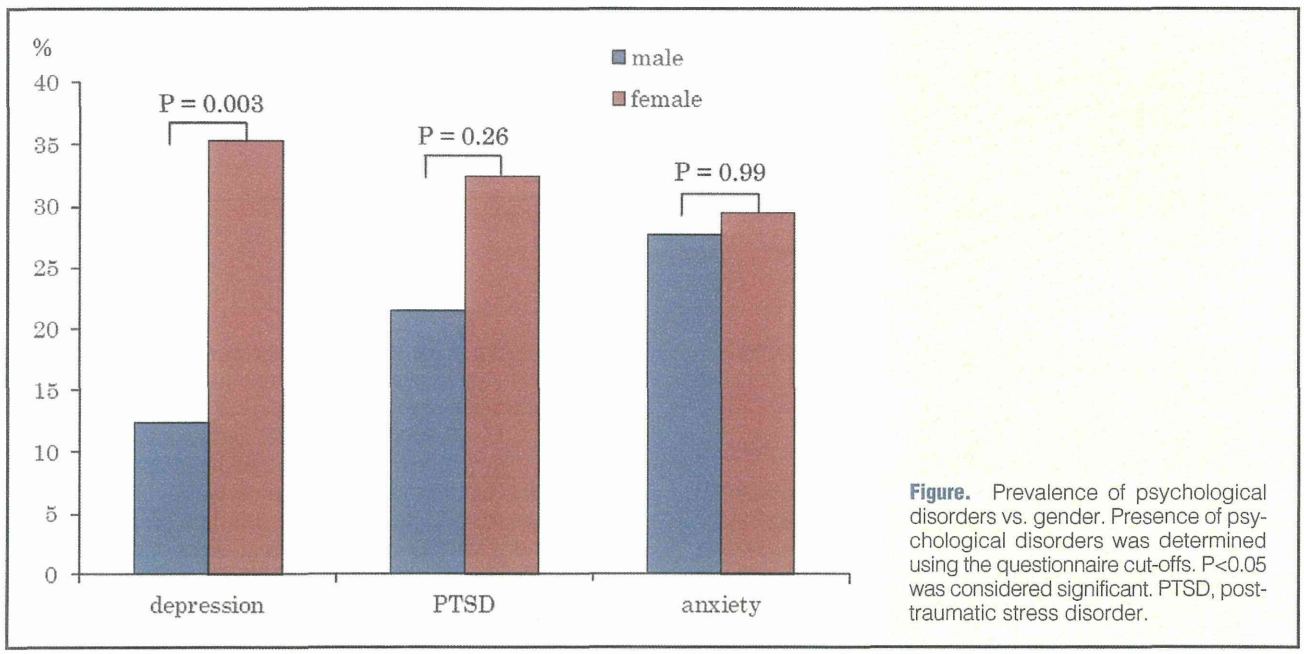

Figure. Prevalence of psychological disorders vs. gender. Presence of psychological disorders was determined using the questionnaire cut-offs. P<0.05 was considered significant. PTSD, post-traumatic stress disorder.

respondent experiences the problem. Items 7, 20, and 26 were phrased in positive terms to avoid a response bias. WAICD score is the total of 26 items, with a score range of 0–104. Lower scores are reflective of less worry, whereas higher scores are indicative of heightened worry.[26] Cronbach's α of the Japanese version of the WAICD used in this study was 0.89, indicating that it is a valid and reliable instrument.

All of the questionnaires were completed in one-to-one interviews. The interviewers asked the questions given in the questionnaires while recording the conversation, then filled in the answers on behalf of the patients.

Statistical Analysis

Data were analyzed using SPSS 20.0 (SPSS, Chicago, IL, USA). Discrete variables were compared with the chi-square test (Fisher's exact test when appropriate) and continuous variables with Student's t-test for independent samples (Mann-Whitney U-test as an alternative). Mean±SD was calculated for continuous variables, while frequencies and percentages for used categorical variables. One-way multivariate analysis of variance (MANOVA) was performed to examine the relationship between gender and health-related QOL (as measured by SF-8 subscales), and gender and psychological factors, respectively. Hierarchical multiple regression analysis was used to analyze how well the independent variables were able to predict the occurrence of psychological disturbances and decrease of QOL. Suyama-Chishaki et al found that female patients and older ICD patients tended to have limited QOL and poor performance on psychological measures.[5] Sears et al also found that age, female gender, and defibrillation shock were